EUROPEAN ORGANIZATION FOR NUCLEAR RESEARCH
ORGANISATION EUROPEENNE POUR LA RECHERCHE NUCLEAIRE

CERN – PS DIVISION

PS/ RF/ Note 97-23 (MD)

DIAGNOSIS OF LONGITUDINAL INSTABILITY IN THE PS BOOSTER OCCURRING DURING DUAL HARMONIC ACCELERATION

A. Blas, S. Koscielniak and F. Pedersen

Abstract

The aim of the machine development sessions described in this note was to determine the type of instability involved when using the second harmonic cavity; and to explore the phenomenology of the instability under different conditions (e.g. beam intensity, cavity voltage-ratio and phase difference).

Geneva, Switzerland
9 January 1998

BOOSTER MACHINE DEVELOPMENT 14-16 July 97

Contents

1 Introduction

Since its introduction in the Cern PS Booster in 1982, the dual harmonic acceleration process suffers from an unexplained instability occurring when the second harmonic cavity is controlled by the first harmonic gap signal. An empirical solution, still in use, was found by L. Magnani **[1]** using the beam fundamental component as a phase reference for the second harmonic cavity voltage.

The aim of the machine development sessions described in this note was to determine the type of instability involved when using the second harmonic cavity; and to explore the phenomenology of the instability under different conditions (e.g. beam intensity, cavity voltage-ratio and phase difference).

1.1 Principle of measurements

The behaviour depending on whether the second harmonic is synchronised to the beam or cavity phase is of primary importance. Switching between these two possibilities for the control signal and watching the ensuing behaviour of the beam was the main principle of the measurements.

The type of beam instability was monitored on an oscilloscope with mountain range capability and also on a mode monitoring system **[2]** set to measure the n =0, m = 1,2,3,4, or 5 side bands around the second harmonic of the rf frequency. The mode analyzer gives a signal proportional to the **multipolar amplitude**.

We also attempted to make some comparison of **growth rate** when switching from beam to cavity synchronisation (stable to unstable position) under various conditions of intensity, voltage, phasing, control gains, etc.

1.2 Regulation/Control technologies

We tested the behaviour of the system with different beam control technologies: The first one is the so called **"analogue beam control"** that makes use a PLL (phase locked loop) with an analogue VCO (voltage controlled oscillator), one for each cavity. The particularity of such a technology is that each VCO needs an input integration to avoid a phase lag increasing with the RF frequency.

In a second step, we tested a **mixed beam control**: digital for the first harmonic and analogue one for the second harmonic.

The last step was to use a **digital beam control for both cavities.** In this case the second harmonic rf synthesizer is fed directly with the digital word from the first harmonic synthesizer, resulting in a synchronised rf progression (we suspected a sort of high frequency excitation due to transitory phase differences).A feature of this system is that there is no need to use an integrator in the phase loop to eradicate d.c. error in the RF.

1.3 Conclusions

In such a lengthy document, it is always of benefit to the reader is the conclusions are given immediately, and this what we propose to do.

1.3.1 Sextupolar instability

In sections 2.1 and 2.2, we conclude there is very strong evidence for a longitudinal sextupole mode instability (m=3, n=0). This occurs when the cavities are anti-phased and the SHC signal comes from the gap fundamental. The coherent frequency is approximately $3f_s$, and the overlay of bunch shapes displays 3 nodes.
There is no evidence of a dipole (m=1) or decupole (m=5) instability.

In section 3.1 we conclude the instability is self-stabilized by the acquisition of bunch tails, and the appearance of a discontinuous derivative at $\pm 90^{\circ}$.

1.3.2 Beam intensity

The instability shows almost **no dependence** on beam current (section 3.2). From this we conclude that the instability is not due to an "impedance", nor to beam loading, nor to space-charge.

1.3.3 Cavities in-phase

There is no beam instability when the cavities are in-phase, the so-called "short bunch mode". Though the beam is changed (from long to short) none of the control loops are changed (except the reference setting of φ_2), from which we conclude the **instability** is **intrinsic to** the **beam** (albeit modified by the interaction with loops).

1.3.4 Analogue versus digital

This instability is only **weakly dependent** of whether the beam control is all analogue (section 3) or all digital (section 4), or a mixture. Growth rate appears slower with all digital control.

1.3.5 SHC gain

In sections 2.4 and 4.4, we conclude the instability growth rate increases when the SHC gain is reduced.

1.3.6 Voltage and phase

The **dependence** on voltage and phase relationships between fundamental and 2^{nd} harmonic is **complicated** (sections 3.4 and 4.4). With V_2 50% of V_1 instability occurs for $\varphi_2 > 150^{\circ}$. With V_2 30% of V_1 instability occurs for $\varphi_2 > 160^{\circ}$. With V_2 20% of V_1 instability occurs only for $\varphi_2 = 180^{\circ}$. Growth rate reduces as V_2 reduces.

1.3.7 Short bunches

Section 5.1 indicates small emittance bunches (made by longitudinal scraping) are stable when the cavities are anti-phased (bunch length 150^0 FW).

2 Diagnosis of sextupole mode

Monday 14th July: at 9:0 a.m. all machine cycles were in use and so, initially, measurements were made parasitically. At 11:00 a.m. an MDAD cycle became available, allowing potentially beam destructive tests to be made. Tests were made with the standard analogue control, and the order of 7x10^12 protons per pulse.
The second harmonic corrector (SHC) signal can come from the beam or cavity fundamental ("gap"). Normally, the signal is from the gap during injection and then switches to beam for acceleration; and this gives stable operation. In order to see the instability, we chose to switch back (from the beam) to the cavity signal. The value BAX.ORF2 => start signal from gap, and BAX.ORF1 => start signal from beam.

2.1 Frequency of instability

The instability is manifest as beam loss and fall of the beam current (Idc) signal. We also observed the beam phase loop signal ($\Phi b,s-\Phi rf,s$) during the instability, and using the frequency analysis feature of the Tektronix digital oscilloscope noted the dominant frequency of 12 kHz (see Fig.2.1). This frequency is 3 times the synchrotron frequency during dual harmonic operation, and very suggestive of the instability being due to a beam sextupole mode.

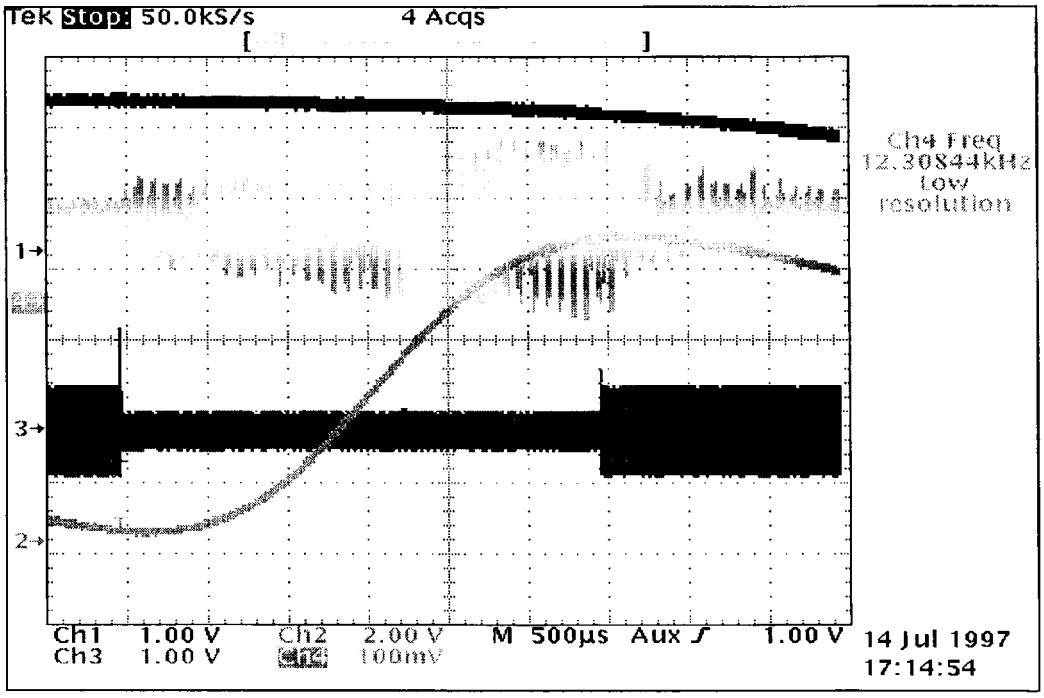

Figure 2.1 Zoom of Fig.2.2 for frequency measurement. **Trace 1** shows the falling beam current, **Trace 4** shows the 1st harmonic phase loop signal.

Rack 716 contains a "Mode Analyzer" [PS/BR Note/77-10] which performs peak detection on a signal with a given frequency. Essentially, this allows to see the amplitude versus time evolution of signals at f_s, $2f_s$ $3f_s$, $4f_s$, $5f_s$, etc.. The mode analyzer was used at $3f_s$ and gave the results of Figure 2.2.

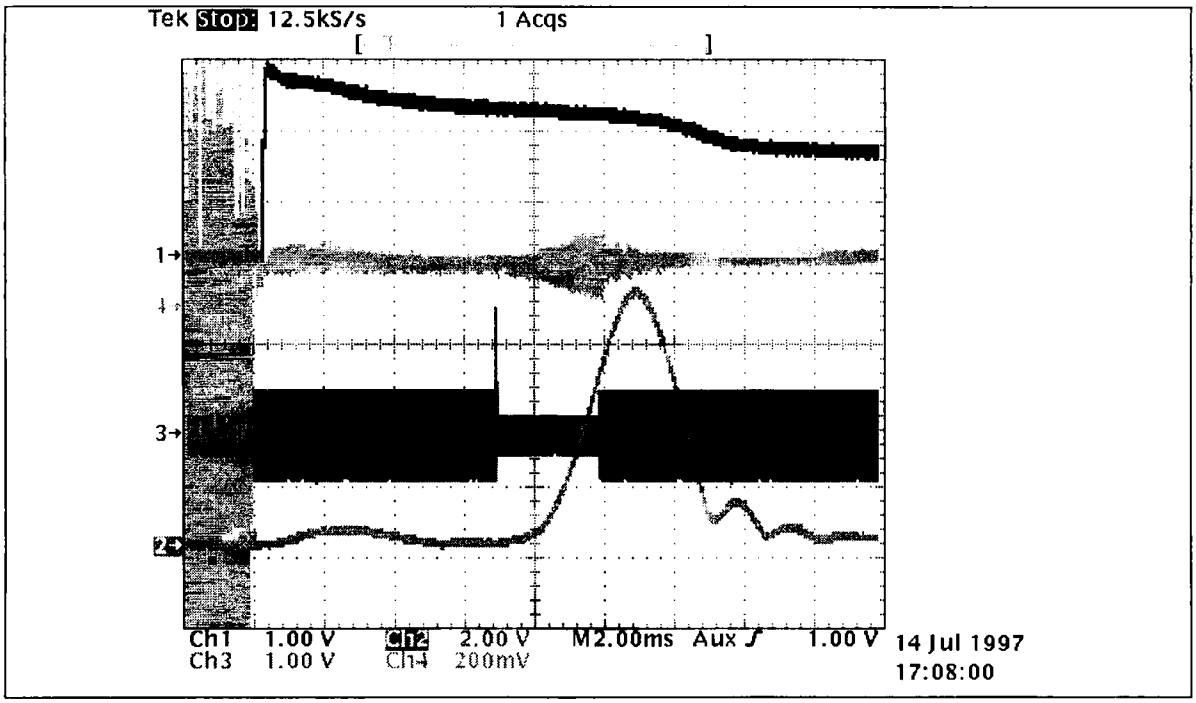

Figure 2.2 Oscillogram of PS Booster parameters for instability diagnosis.
Trace 1: beam current 4E12protons/V, **Trace 2**: amplitude of m=3, n=0 mode,
Trace 3: gap-beam-gap commutation, **Trace 4**: (Φb,s-Φrf,s) of 1st harmonic.

The mode analyzer was also used at $1f_s$ and $5f_s$ (Figures 2.3 and 2.4) but there was no discernible growth of the dipole or 5-pole beam modes after the beam-gap commutation. (There is a dipole component after injection, but this dies away before the switching).

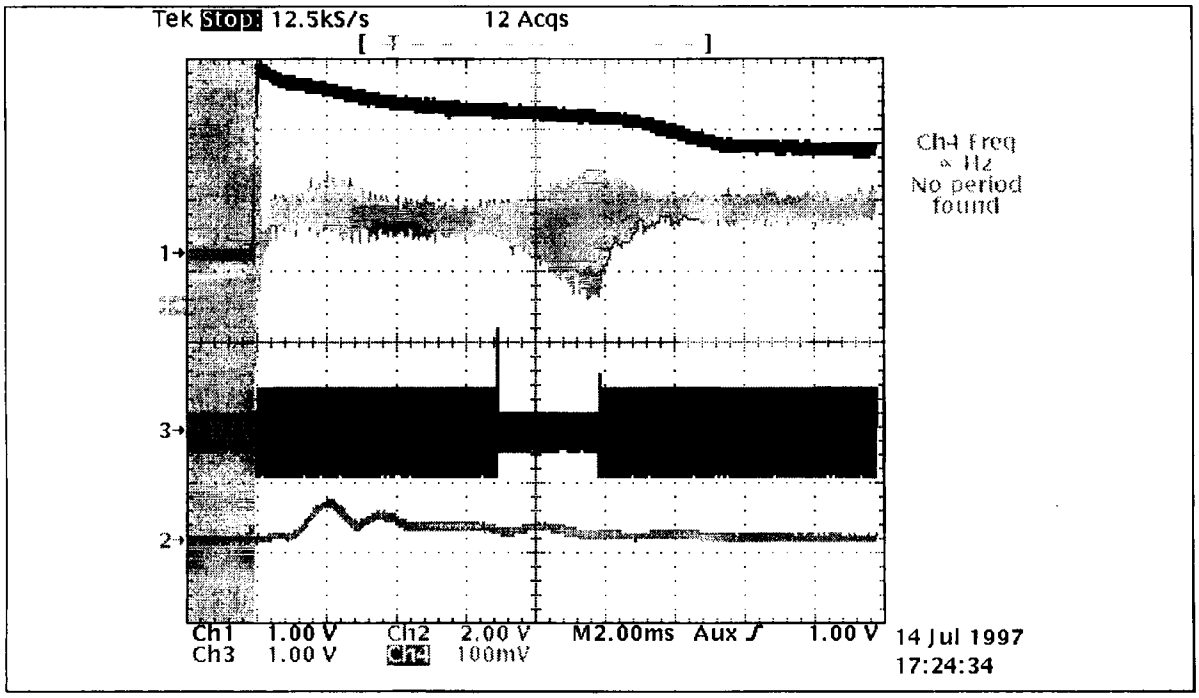

Figure 2.3 As for Fig.2.2, but trace # 2 monitored at dipole frequency.

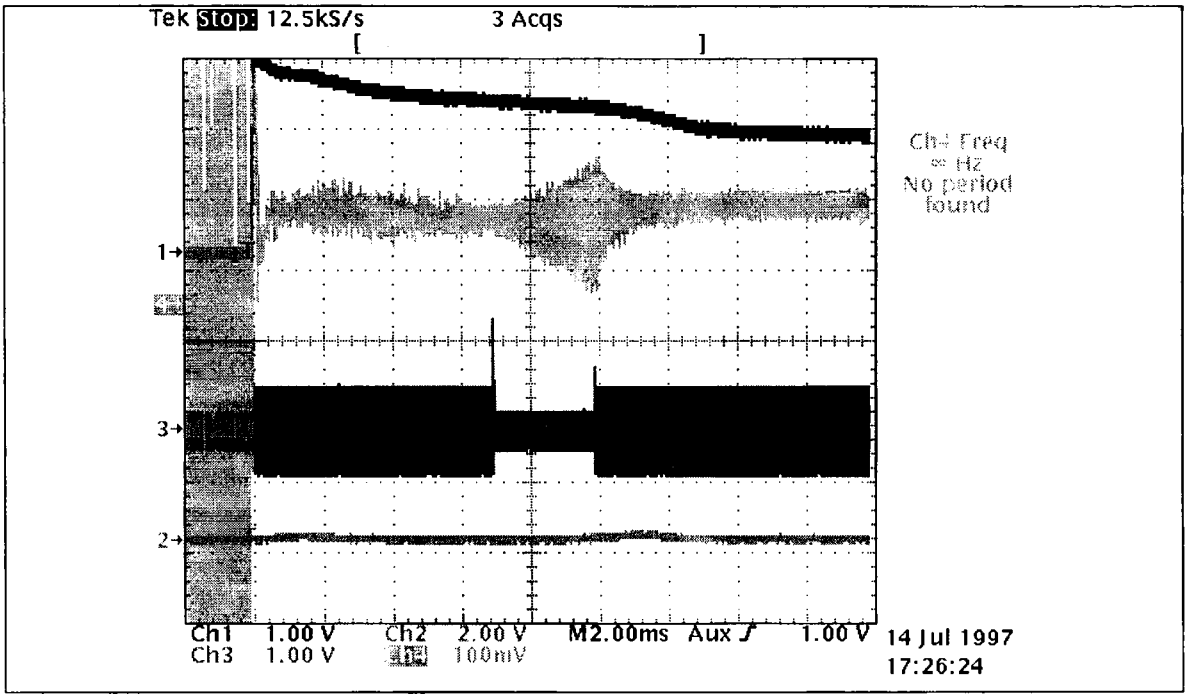

Figure 2.4 As for Fig.2.2, but trace # 2 monitored at decupole frequency.

2.2 Bunch shapes

We realized that further evidence of a sextupole mode could be obtained from mountain range plots of the bunch shape versus revolutions (i.e. time).
Rack 709 contains a Tektronix oscilloscope set up for just such an observation; it also allows for overlay of bunch shapes without a staircase offset.

The frequency of the main perturbation was also measured directly from the beam mountain range pictures The period of oscillation should be 50 turns (frev/fs=3/5 MHz/12kHz). The bunch shape was sampled every 5 turns, and a periodicity of 50 turns was confirmed.

The mountain range display was suggestive of a sextupole mode, but not unambiguous; it could have been a dipole mode. However, if one does a simple superposition of the bunch shapes (sampled once each revolution) then the number of nodes in the overlays indicates the azimuthal mode number (m=1,3,5, etc.). **The overlays**, Figures 2.5 and 2.6, **have 3 nodes** which is further confirmation of a sextupole mode.

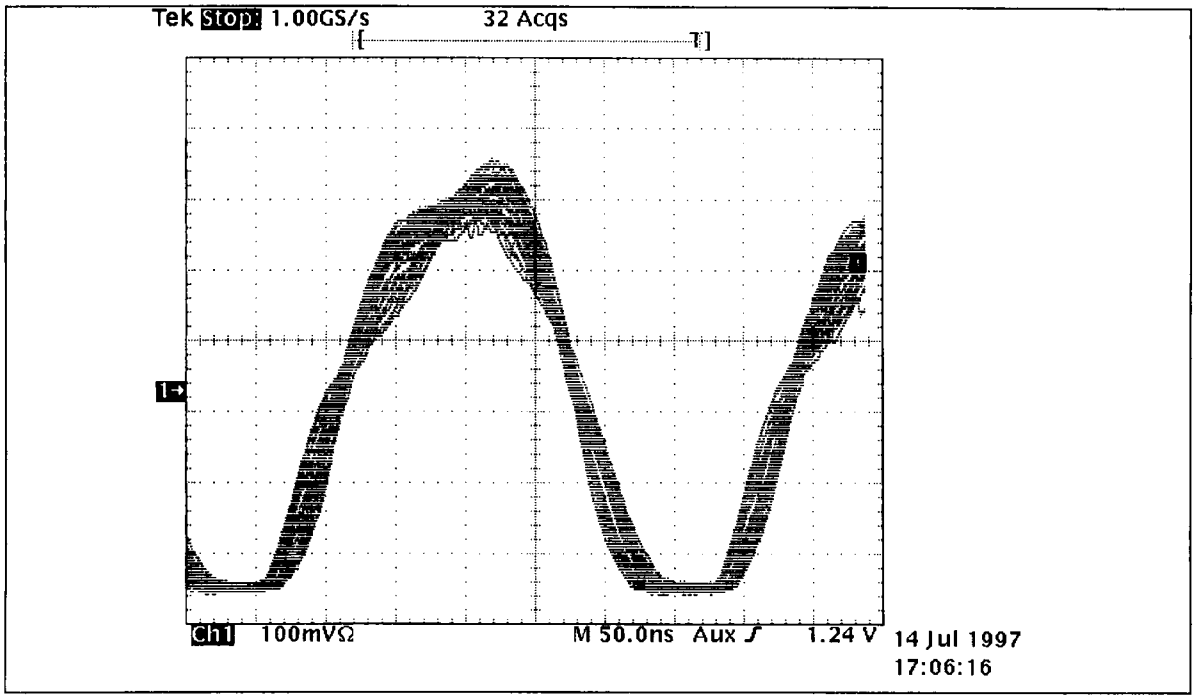

Figure 2.5 Overlay of bunch shapes starting at 206 ms, scan each 10 revolutions during 500μs – shows 3 nodes.

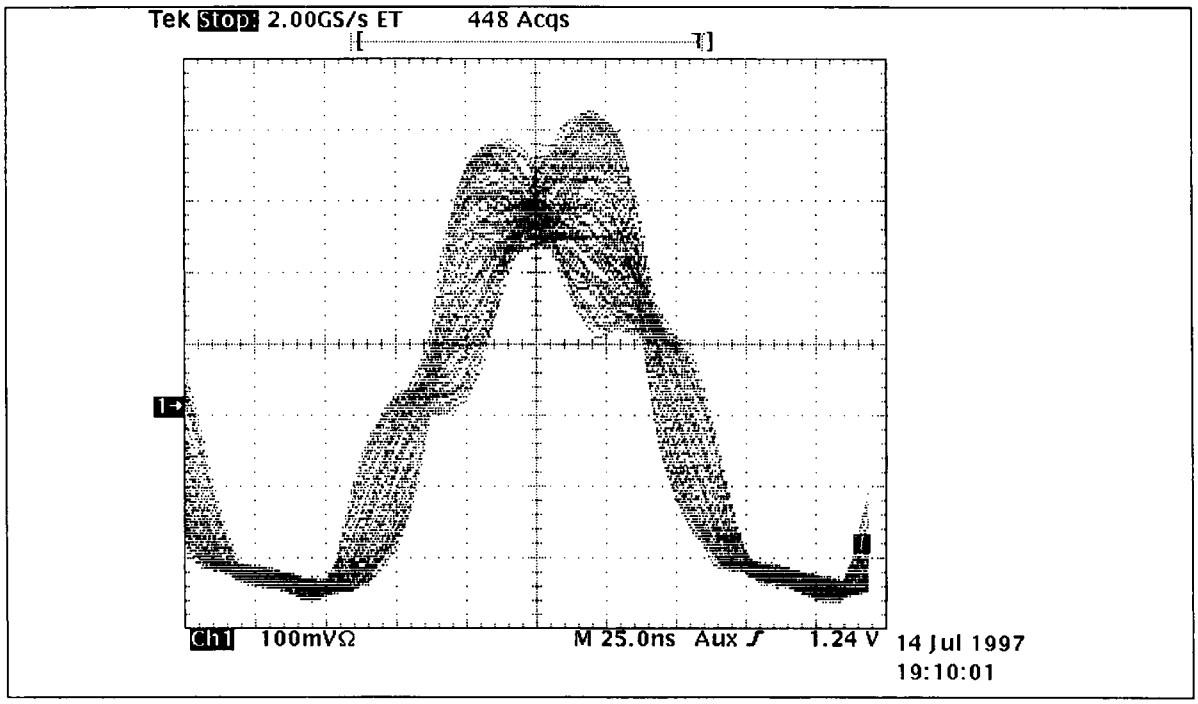

Figure 2.6 Overlay of bunch shapes starting at 236 ms, scan each 5 revolutions during 500μs – shows 3 nodes.

2.3 Attempt to vary parameters

At noon, an attempt was made to see what is the effect of space-charge on the instability by making measurements at a 1 GeV flat top. Unfortunately, this attempt was

"sabotaged" by the synchronization loop which (at ejection) locks the Booster RF to that of the CPS.
In the afternoon, an attempt was made to find the influence of altering various parameters (e.g. phase lop gain, beam intensity, etc.) on the growth of the sextupole mode (as measured by the amplitude versus time from the "mode analyzer"). This attempt was unsuccessful because of the very poor repeatability. Essentially, at the moment of "switching the SHC signal from beam to cavity" we could not prepare beams in identical initial states.

Essentially, we had let the instability grow from noise
We also tried to excite the phase loop (1^{st} harmonic) with a perturbation at the frequency of concern (≈10 kHz) but this did not lead to any better results and also excited a coupled-bunch instability.
We tried to excite the mode by the same method while in the stable position but this also led to insignificant sensitivity to gain adjustments.

2.4 Refinement of procedures

Tuesday, 15^{th} July. Free cycles for MD became available, and we used a modified TSTPS cycle (with acceleration up to 220 ms followed by a flat top) for measurements. The problem with "non-repeatability" encountered the day before was due to ill-determined value of (Φb,s-Φrf,s) at the time of SHC commutation. Blas devised a procedure to ensure a constant given phase difference at the moment of commutation.
The excitation law of the Booster quadrupole magnets does not automatically follow the bending magnet field law; with the consequence that the betatron tune changed significantly during our flat top, leading to beam loss. With the help of Mats Lindros, the Qβ program was adjusted to match the flat top at 100 MeV.
We attempted to prepare a beam of known, consistent state by exciting the beam at 10kHz. In order to do this we had to turn off the coupled-bunch feedback; but this lead to a severe instability and the attempt was abandoned. Consequently, during our measurements, the coupled-bunch mode and quadrupole mode feedbacks were enabled.

Now with the "**soft commutation**" and correct Qβ program we were in a position to make a "variation of parameters" investigation. The synchronous phase was set at zero, and the 2 harmonic components of the RF set in perfect anti-phase. The growth rate at $3f_s$ was observed using the "mode analyzer".

2.4.1 Dependency on PLA gain

There was no discernible change in the growth rate when the PLA gain of the 1^{st} harmonic was modified.

2.4.2 Dependency on SHC gain

The growth rate was faster with reduced SHC gain, and the bunch shapes became more distorted also. This test was repeated on Wednesday with rather greater care. Using an all analogue beam control, the SHC gain was reduced (5 turns less than nominal on the circular Vernier gain knob of the SHC) substantially, and the sextupolar instability appeared before commutation (i.e. while beam signal still being used for control). This is shown in Figure 2.7.

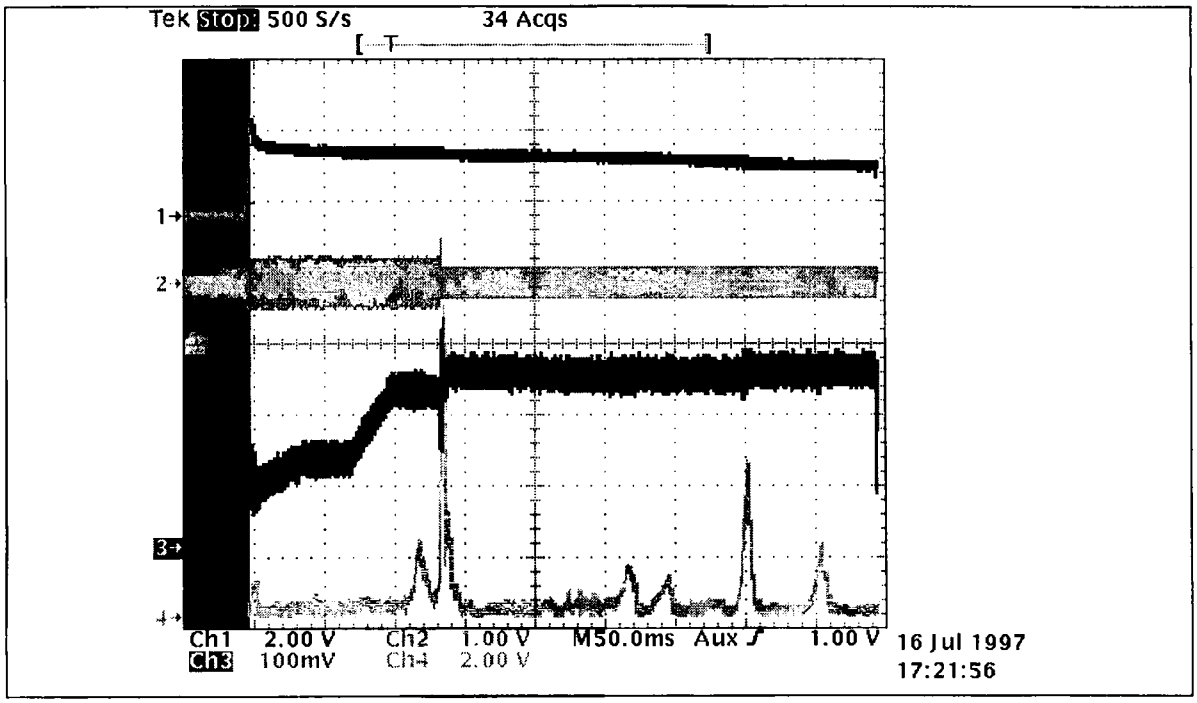

Figure 2.7 Oscillogram as for Figure 3.2, with analogue control and much reduced SHC gain. Trace #4 shows the mode analyzer signal at $3f_s$=9.7 kHz, and an instability starting to rise before the commutation at C170. This results in the beam loss recorded in trace #1.

2.4.3 Short bunch mode

With the two RF components in phase (the so-called "short bunch" mode of operation), the instability disappears. This was confirmed in more detailed measurements reported in section 3.

3 Definitive Measurements

Wednesday 16th July: with the initial "teething problems" sorted out, we were now in a position to make some definitive measurements and record their results.
Using the modified TSTPS cycle, the measurements were executed on a **flat part of the magnetic field** set to 1832 Gauss from 134 to 512 ms after injection.
The first cavity was set to 10 kVolts and the second to 5 kV during all the cycle (c08=10,C16=50). Initially, we used an **all analogue beam control**.
Commutation was made at C170 (injection = C35 = 35 ms after C0.

3.1 Long bunch mode

Initially, used all analogue beam control. With the parameters of the TSTPS cycle (different from Mondays settings), the instability frequency changes. The frequency was measured from the beam phase loop signal (Φb,s-Φrf,s) using the Tektronix digital scope, and found to be approximately 9.5 kHz.

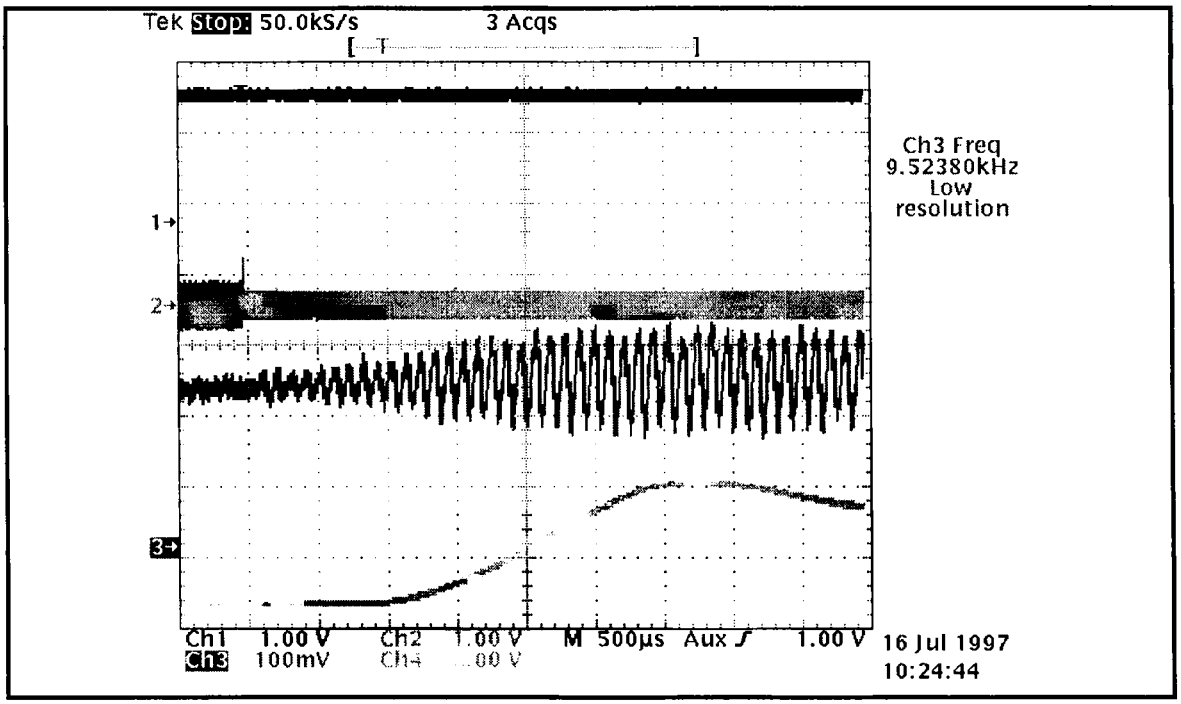

Figure 3.1 Zoom of fig 3.2; trigger point = C170, $\varphi_2 = 180^\circ$ (square bunches)

Trace 1: DC beam current 4 E12 p/V
Trace 2: rf reference beam to gap switching (gap = low amplitude signal)
Trace 3: First harmonic phase error (beam to cavity) measurement (= $\Delta\Phi$)
Trace 4: m = 3, n = 0 mode measured at 3 f_S = 9.7 kHz.

Using the mode analyzer, and varying the observation frequency, the mode amplitude was maximized at 9.7 kHz which is 3 f_s.
Figure 3.2 shows (trace # 4) the growth of the instability at 3 f_s following commutation at C170.

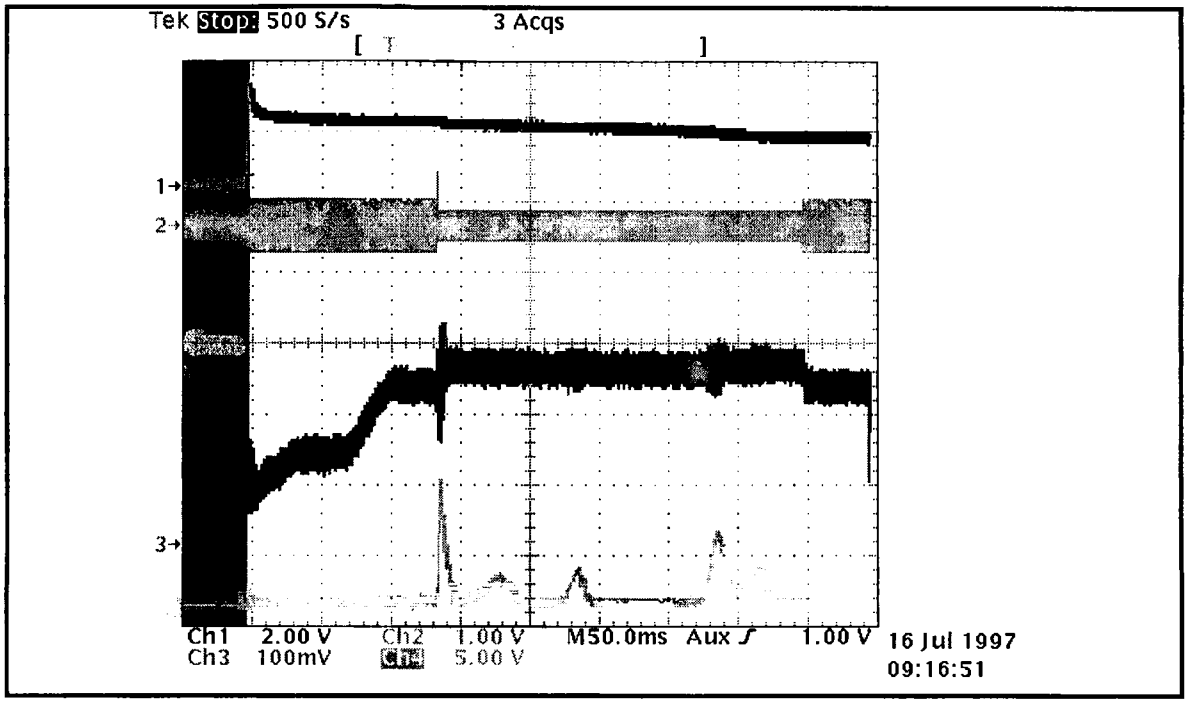

Figure 3.2 Oscillogram , trigger point = C35, $\varphi_2 = 180^\circ$ (square bunches)

Trace 1: DC beam current 4 E12 p/V
Trace 2: rf reference beam to gap switching (gap = low amplitude signal)
Trace 3: First harmonic phase error (beam to cavity) measurement (= $\Delta\Phi$).
Trace 4: m = 3, n = 0 mode measured at 3 f_S = 9.7 kHz with "analyzer".

Note that most of the losses do not appear on the DC beam current measurement while we stay at a constant B field because "out of bucket" particles remain in the vacuum chamber.

Figures 3.3—3.7 show various stages in the evolution of the instability through a sequence of mountain range plots. The bunches are initially 296 degrees long (FW).
In particular, the plots show the following features.
Figure 3.3 shows a rather stable image (at C165) before the SHC commutation (the normal beam behaviour).
Figure 3.4. shows the bunch shapes at the time of commutation (C170).
Figure 3.5 shows the beam 1 ms after switching to the cavity signal; we start to see some sextupolar coherent instability. The instability grows (Figure 3.6) before saturating (Figure 3.7) and stabilising itself.

The **instability is auto-damped** by a complex beam self-arrangement. During this time, the beam distribution function acquires tails and the bunch takes the shapes of figure 3.7. In particular, there is a discontinuity in the gradient at ±67 degrees.

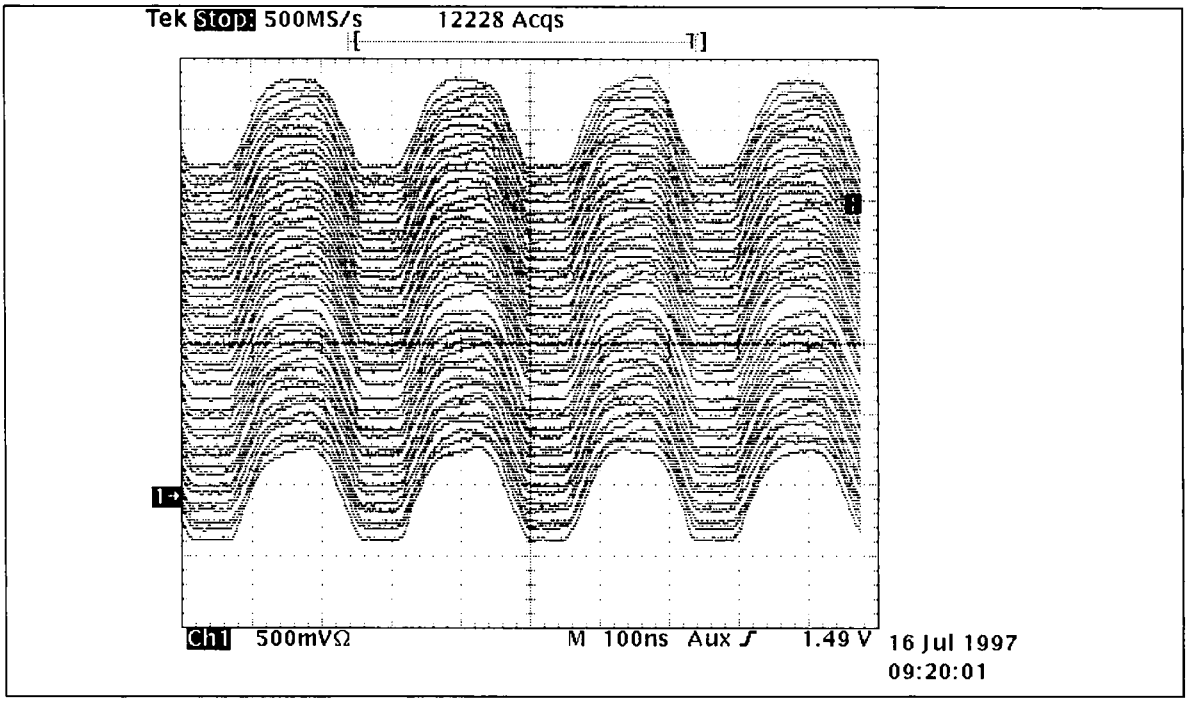

Figure 3.3 Beam signal scanned each 10 revolutions starting from C165 (bottom trace) and lasting 500 μs.

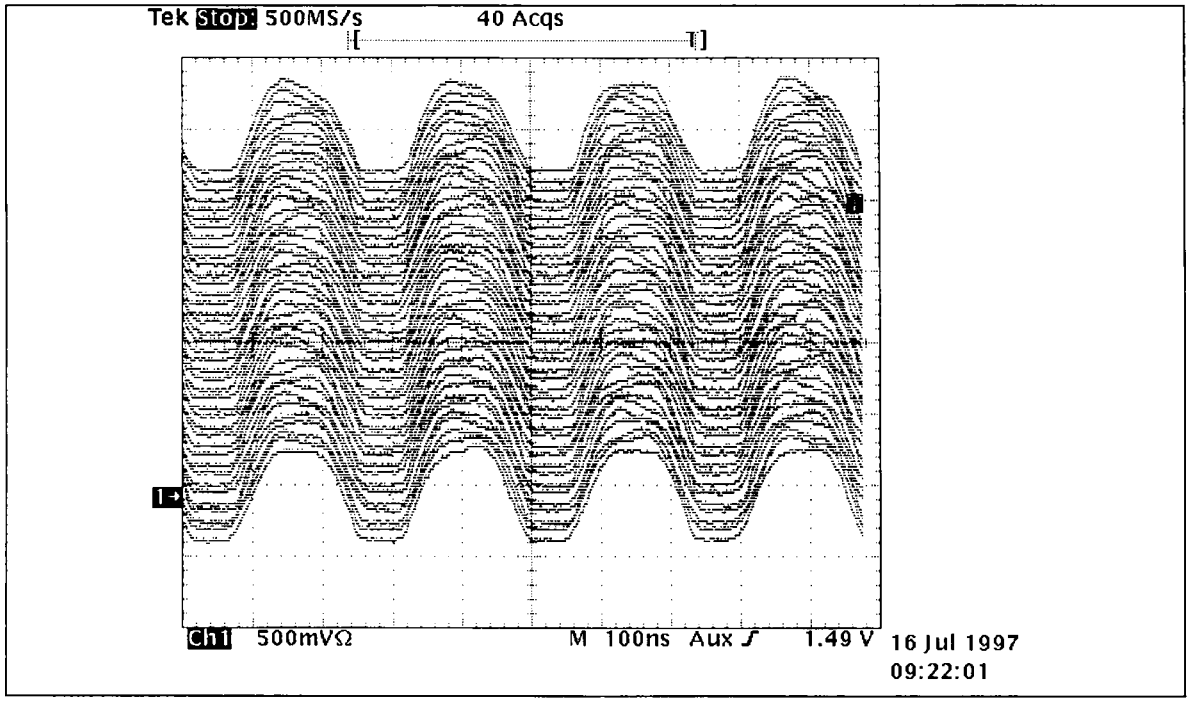

Figure 3.4 Beam signal scanned each 10 revolutions starting from C170 (commutation) as the bottom trace and lasting 500 μs.

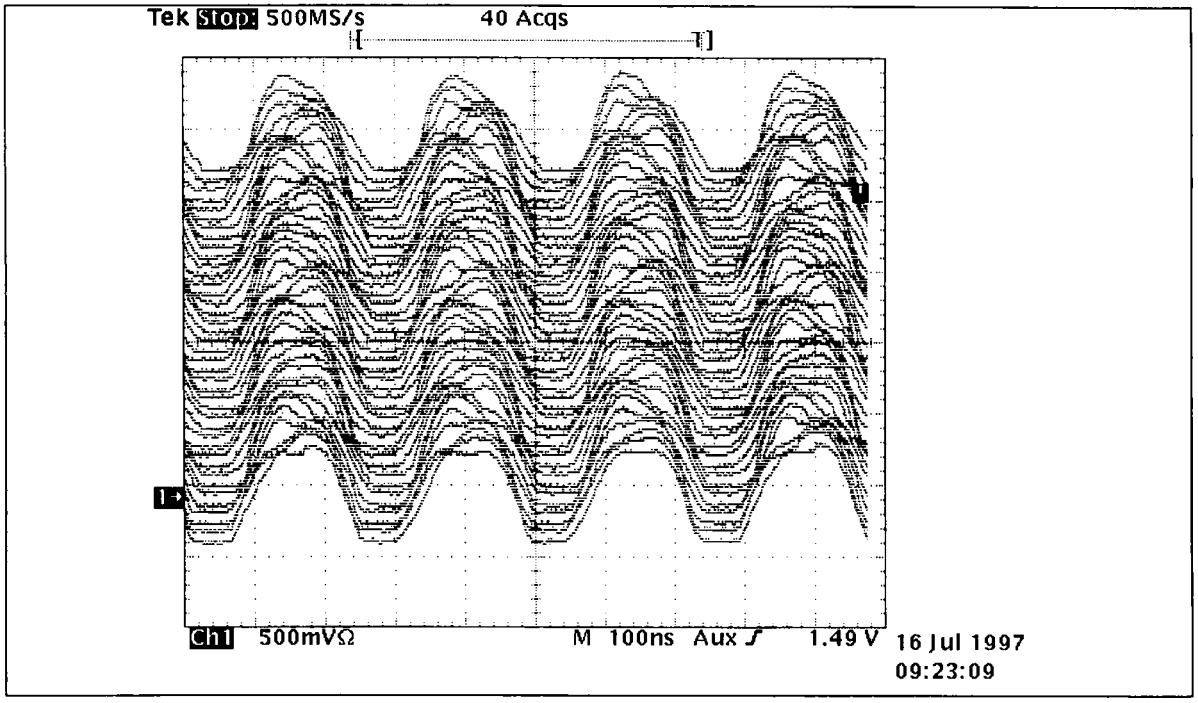

Figure 3.5 Beam signal scanned each 10 revolutions starting from C171 (1 ms after switching) as the bottom trace and lasting 500 μs.

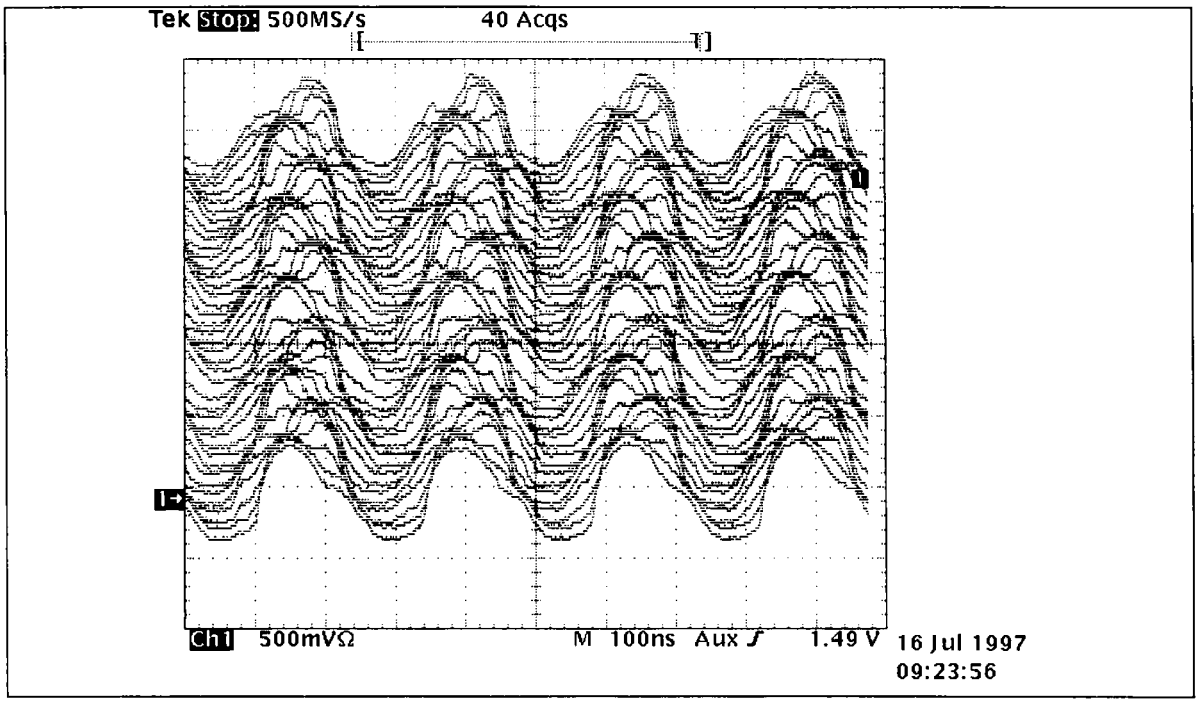

Figure 3.6 Mountain range display of bunch traces once each 10 revolutions starting from C172 (bottom trace) and lasting 500 μs. There is clear sextupolar motion.

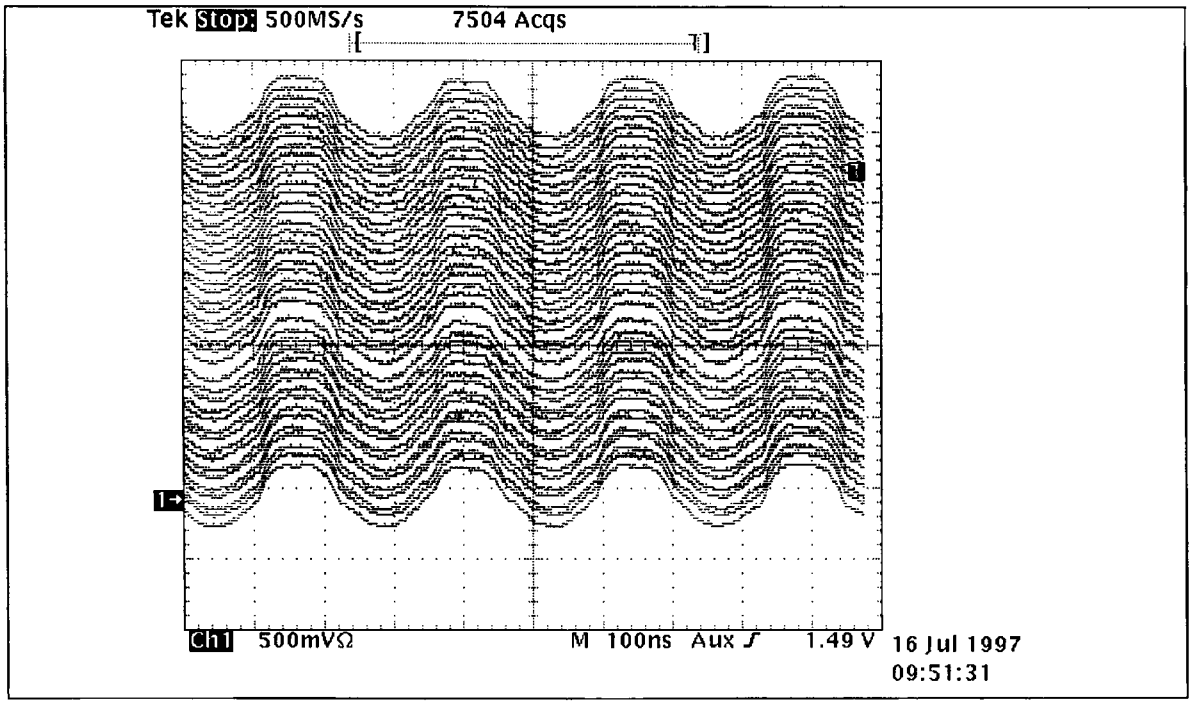

Figure 3.7 Mountain range display of bunch traces each 10 revolutions starting from C195 (bottom trace) and lasting 500 μs. Notice the development of stabilizing tails.

3.2 Intensity dependence

Using the standard set up for long bunch mode (2^{nd} harmonic voltage 50% of fundamental and cavities anti-phased), the beam intensity was varied by changing the number of injected turns from 2 to 21. Below 2 injected turns, the phase loop cannot get enough signal, which leads to an erratic beam control and losses.

For each value of the injection duration, the growth rate was monitored by the mode analyzer set to observe 9.7 kHz. Figures 3.8 through 3.14 indicate almost no dependence on beam current despite an order of magnitude variation of Idc. From this we conclude that the instability is not due to an impedance, nor to beam loading, nor to space-charge.

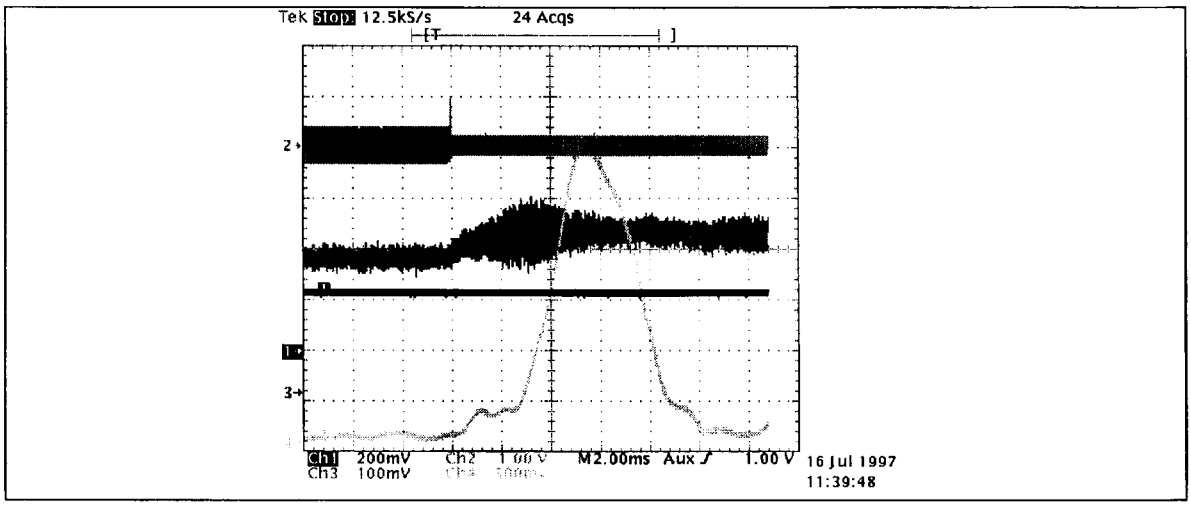

Figure 3.8 Trace 4: Analyzer signal at 3 f_s for 3 injected turns (0.5V/cm) , **Trace 3**: beam phase loop signal, **Trace 2**: commutation signal.

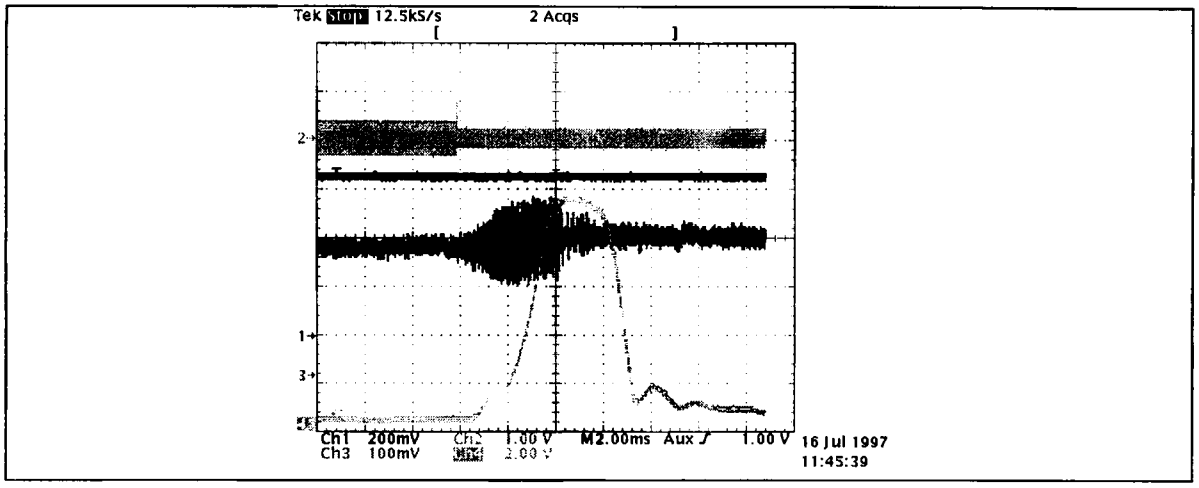

Figure 3.9 Same as Fig.3.8 but analyzer signal at $3f_s$ (trace 4, 2V/cm) for 6 injected turns.

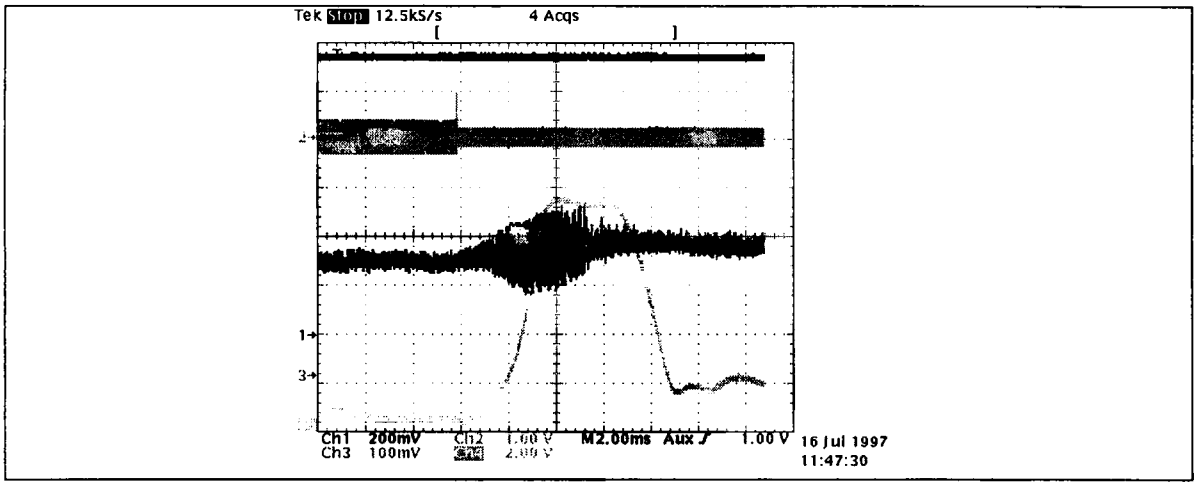

Figure 3.10 Same as Fig.3.8, but analyzer signal at $3f_s$ (trace 4, 2V/cm) for 9 injected turns.

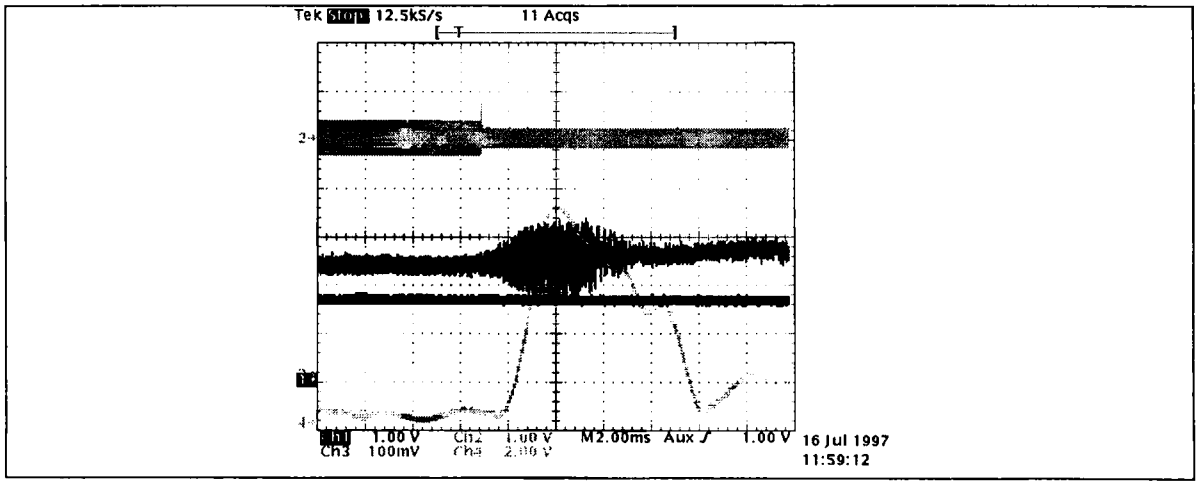

Figure 3.11 Same as Fig.3.8 but analyzer signal at $3f_s$ (trace 4, 2V/cm) for 12 injected turns.

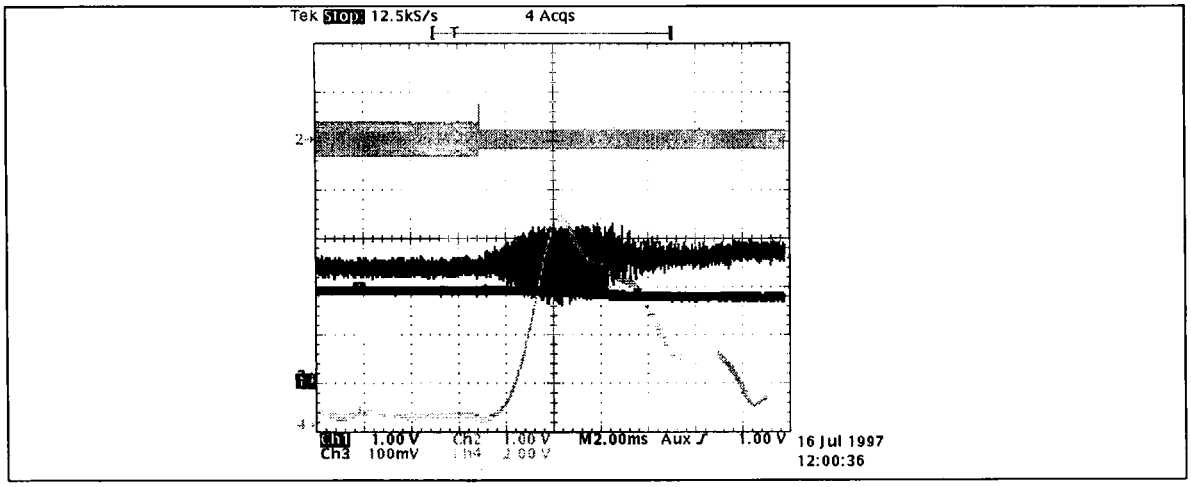

Figure 3.12 Same as Fig.3.8, but analyzer signal at $3f_s$ (trace 4, 2V/cm) for 15 injected turns.

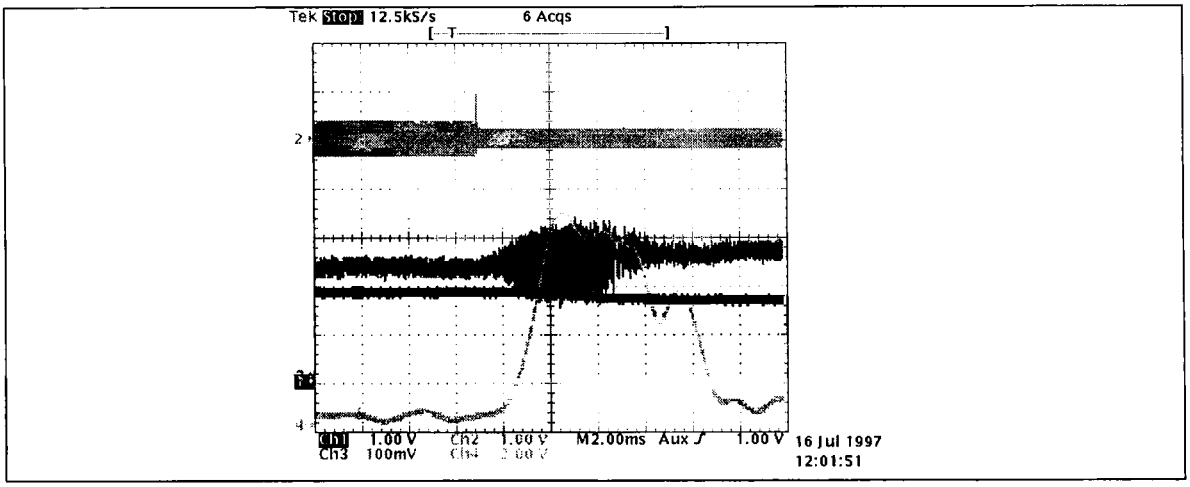

Figure 3.13 Same as fig.3.8, but analyzer signal at $3f_s$ (trace 4, 2V/cm) for 18 injected turns.

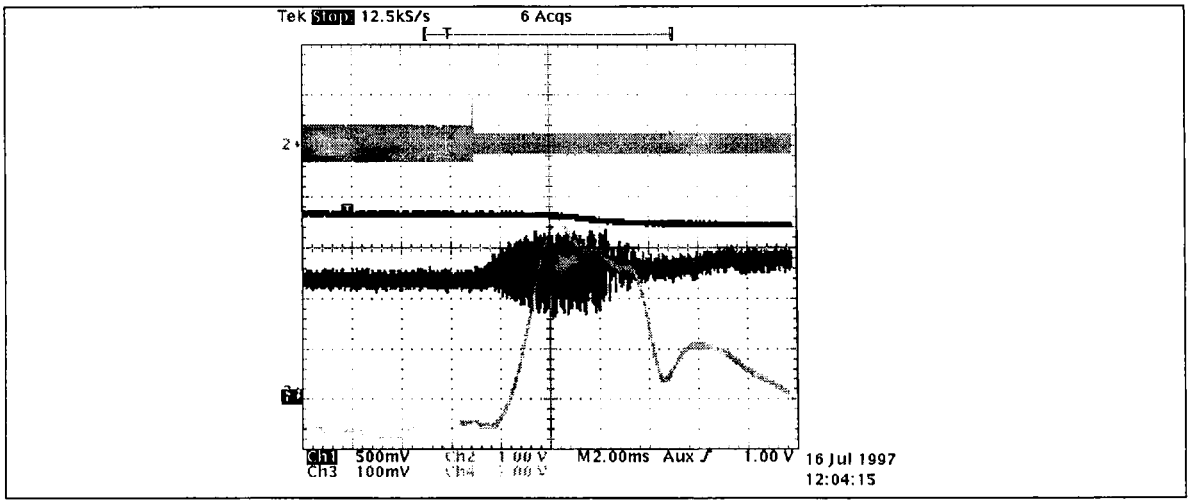

Figure 3.14 Same as Fig.3.9, but analyzer signal at $3f_s$ (trace4, 2V/cm) for 21 injected turns. Losses are due to over-population of the phase-space.

3.3 Short Bunch Mode

Continuing with the analogue control, we now investigated the stability of the short bunch mode of operation, by the same method of commutating the SHC signal from beam to cavity. The results are shown in Fig.3.15. Note the flat mode analyzer trace, indicating no instability. This is confirmed in the mountain range plots of Figs 3.16 and 3.17 taken 5 ms before and after switching at C170. The plots at C170, C171, C172, C195 are identical with Fig.3.17 and are not given. The short bunches are 206 degrees FW.

Note, though we have changed the beam (from long to short) we have not changed any of the control loops (except the reference setting of ϕ_2) or electronics, from which we conclude the instability is intrinsic to the beam (albeit modified by the interaction with loops).

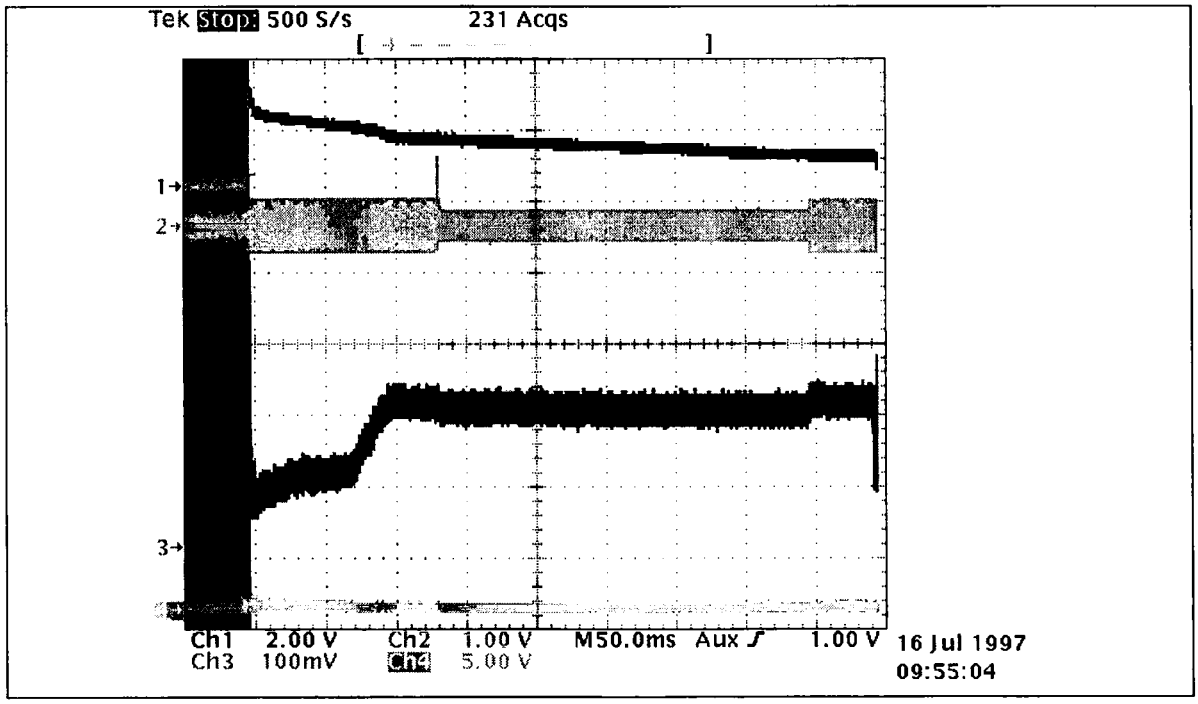

Figure 3.15 Oscillogram. Short bunches (ϕ=0), commutation at C170,

Trace 1: DC beam current 4E12p/V
Trace 2: RF reference beam to gap switching (gap=low amplitude signal)
Trace 3: First harmonic phase error (beam to cavity) measurement ($\Delta\Phi$)
Trace 4: m=3, n=0 mode signal measures at 3 f_s = 9.7 kHz.

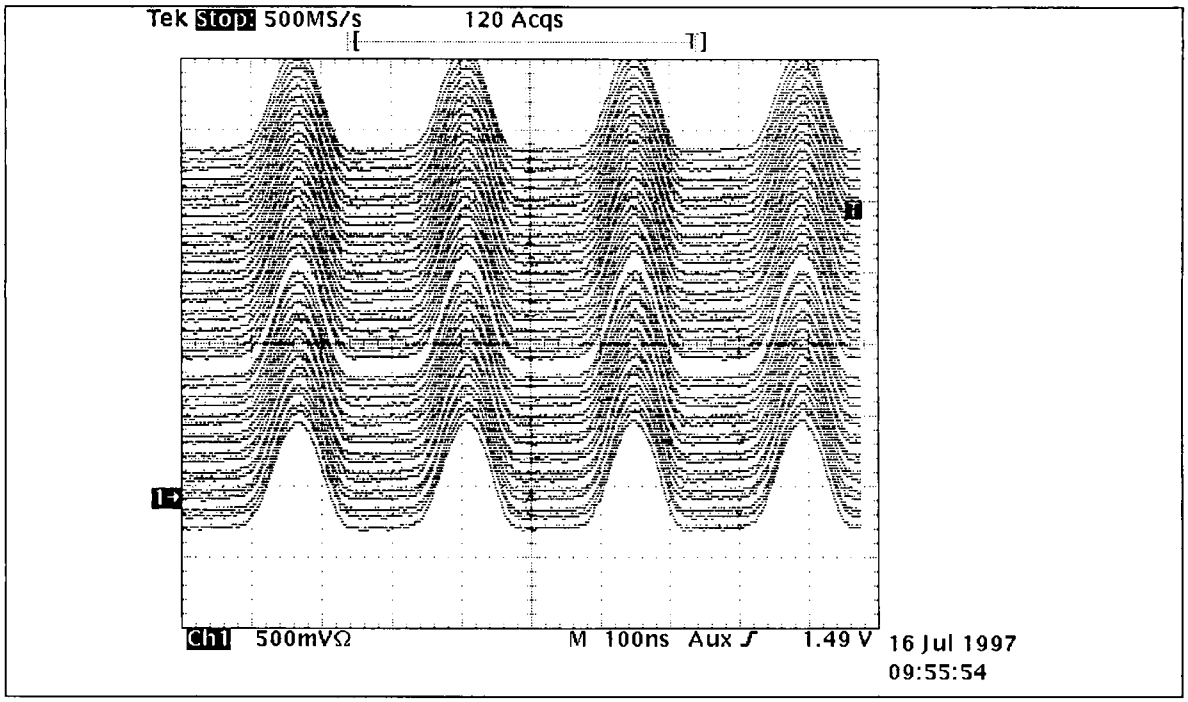

Figure 3.16 Beam signal (short bunch mode) scanned each 10 revolutions starting at C165 (bottom trace) and lasting 500 μs.

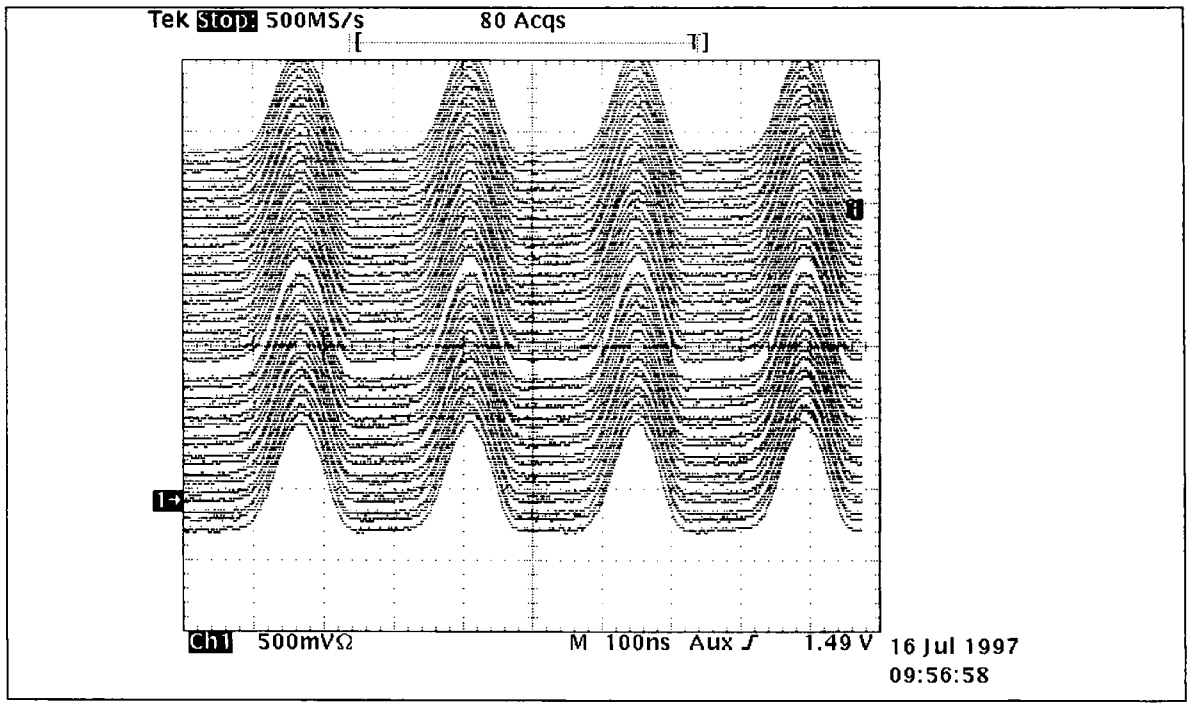

Figure 3.17 Beam signal scanned each 10 revolutions starting from C175 (bottom trace) and lasting 500 μs for $\varphi_2 = 0$. Clearly there is no instability.

3.4 Dependence on Phasing of cavities

With the cavity voltages in-phase, the beam is stable. With the cavities anti-phased, the beam is unstable. Consequently, one expects a "cross-over phasing" at which the instability begins. The use of an arbitrary phase leads to skewed bunch shapes.

The principal of the experiment was to slowly ramp the inter-cavity phasing from 0 (short bunch) to 180 (long bunch) and monitor when the instability starts. The phase program is shown in Figure 3.18, and from the zoom in Fig.3.19 the instability commences at C244 when the phase is 155°. Frequency analysis shows the dominant frequency of the instability to be 9.5 kHz, as shown in the zoom of Fig.3.21.

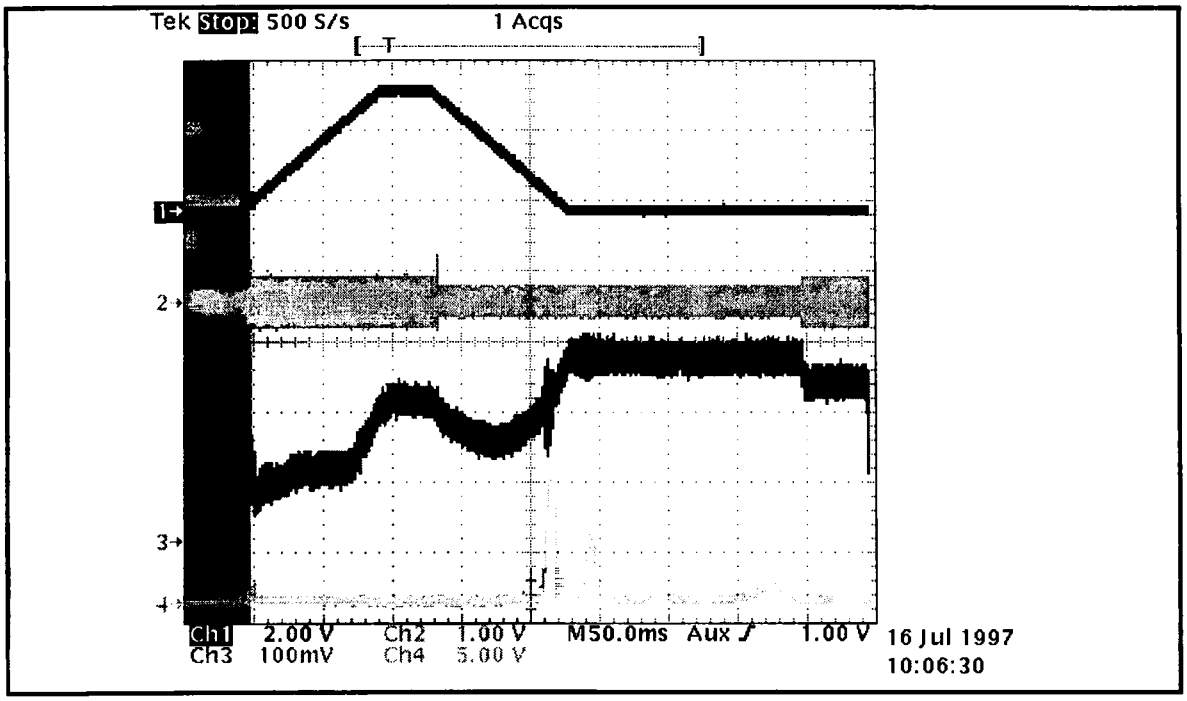

Figure 3.18 Oscillogram. Test with phase shift of cavities, trigger point=C170,

Trace 1:1st to 2nd harmonic phase (bottom = 180, top=0 (short bunch))
Trace 2: rf reference beam to gap switching (gap = low amplitude signal)
Trace 3: first harmonic phase error (beam to cavity) measurement (= $\Delta\Phi$)
Trace 4: m = 3, n = 0 mode measured at 3 f_S = 9.7 kHz.

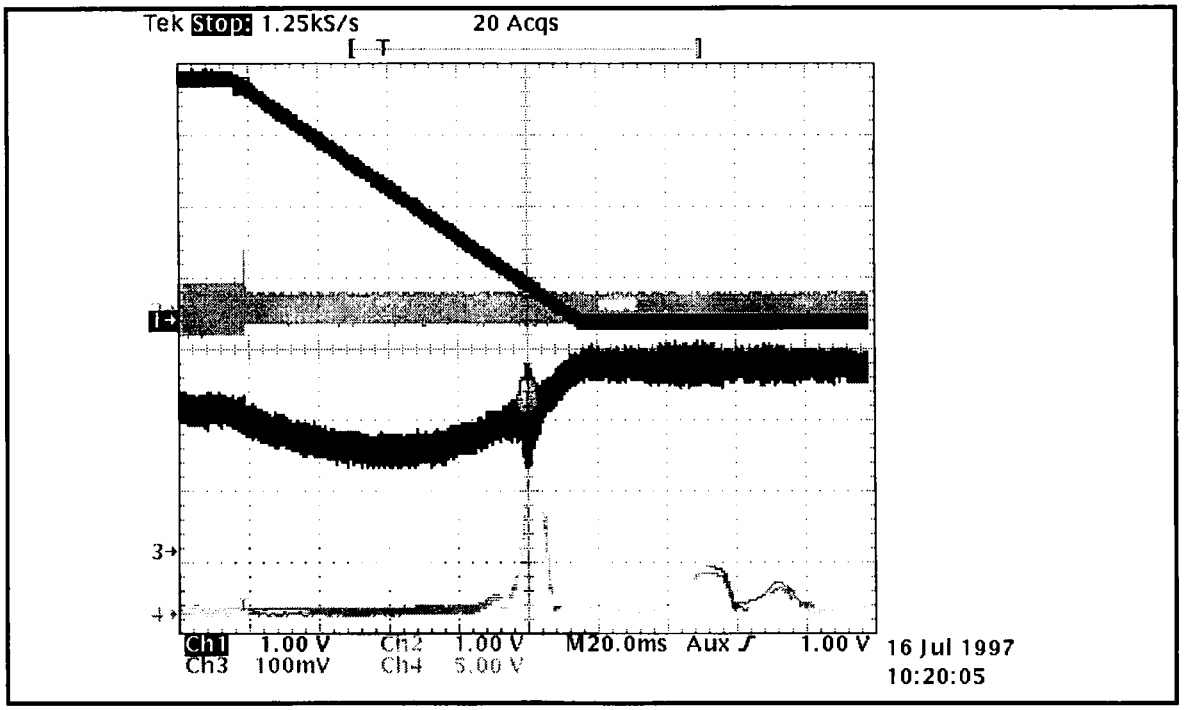

Figure 3.19 Zoom of fig 3.18 trigger point = C170,

Trace 1: 1st to 2nd harmonic phase (bottom = 180, top = 0° (short bunch)
Trace 2: rf reference beam to gap switching (gap = low amplitude signal)
Trace 3: First harmonic phase error (beam to cavity) measurement (= $\Delta\Phi$)
Trace 4: m = 3, n = 0 mode measured at 3 f_S = 9.7 kHz.

3.4.1 Mountain range plots

The mountain range plots of Figures 3.20 to 3.23 show the evolution of the sextupolar instability from its start at C244 towards its saturation at C300. Once more, saturation is associated with the growth of tails in the bunch distribution.
In figure 3.23 the sextupolar perturbation starts to arise quite clearly, and we conclude that when 2nd harmonic is 50% of fundamental that instability occurs for phases ϕ_2 in the range 155-180 degrees.
The bunches are asymmetric because the phase of the two RF components is neither 0 nor 180.

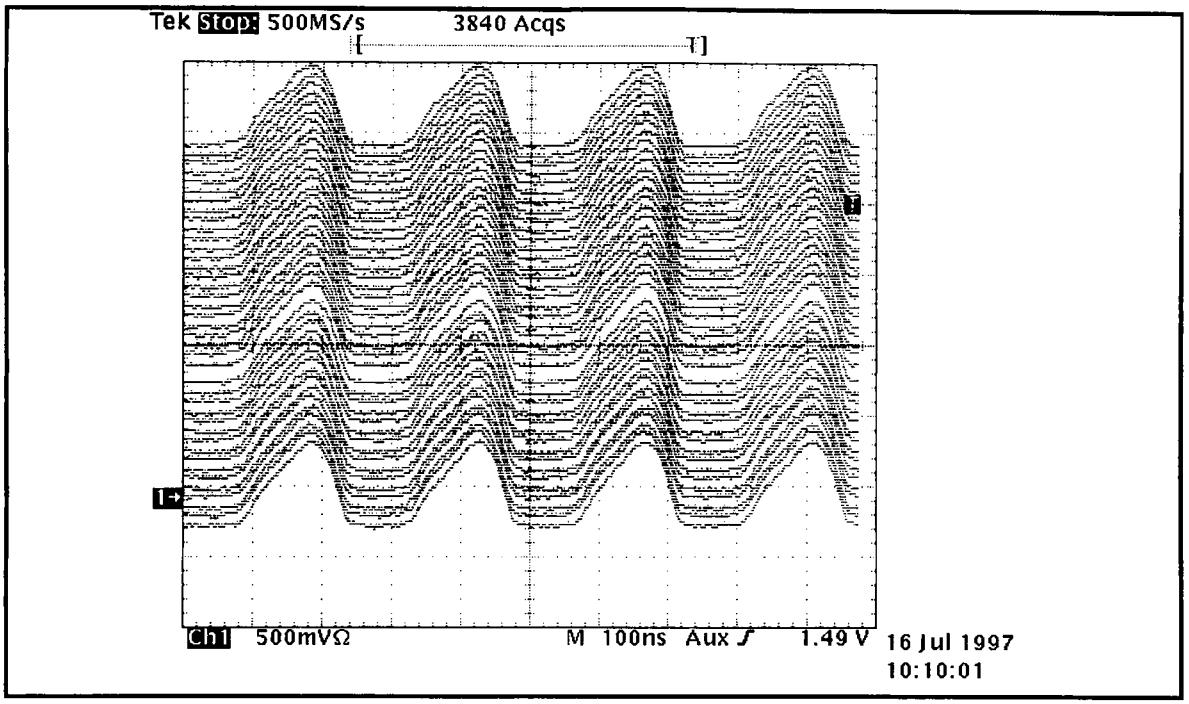

Figure 3.20 Beam signal scanned each 10 revolutions starting from C235 (bottom trace) and lasting 500 μs for φ_2 sliding from 0° to 180°

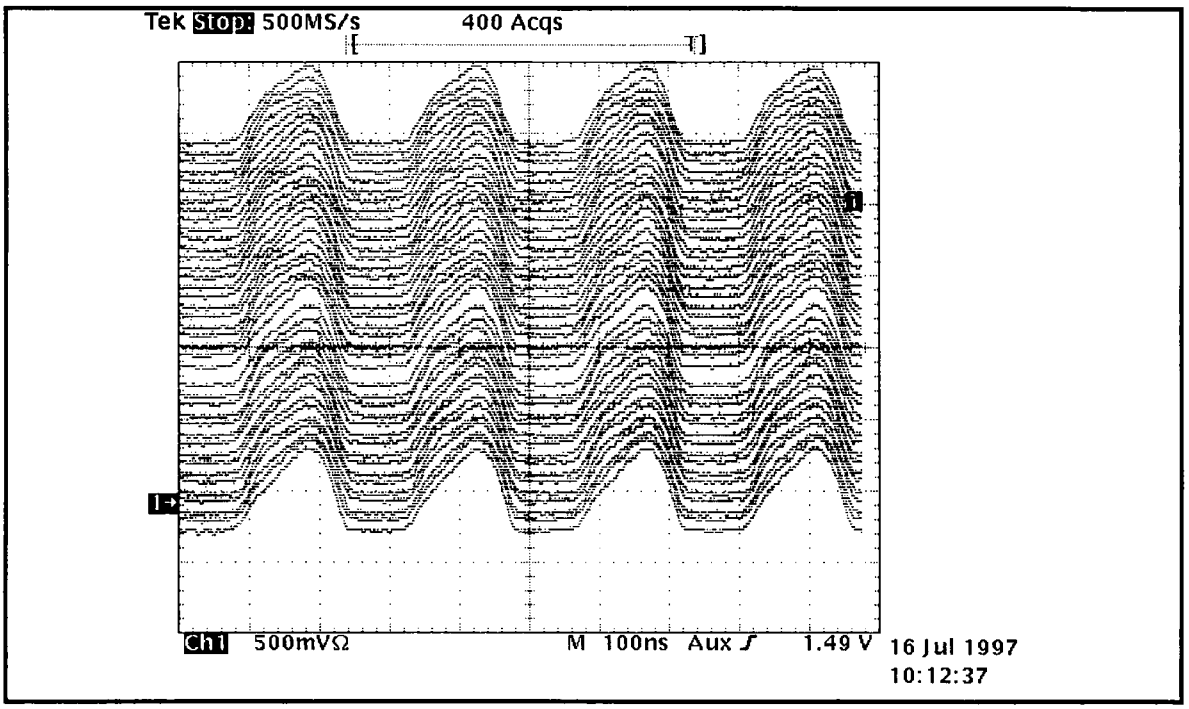

Figure 3.21 Beam signal scanned each 10 revolutions starting from C244 (bottom trace)and lasting 500 μs for φ_2 (phase between 1st and 2nd harmonic RFs) sliding from 0° to 180°

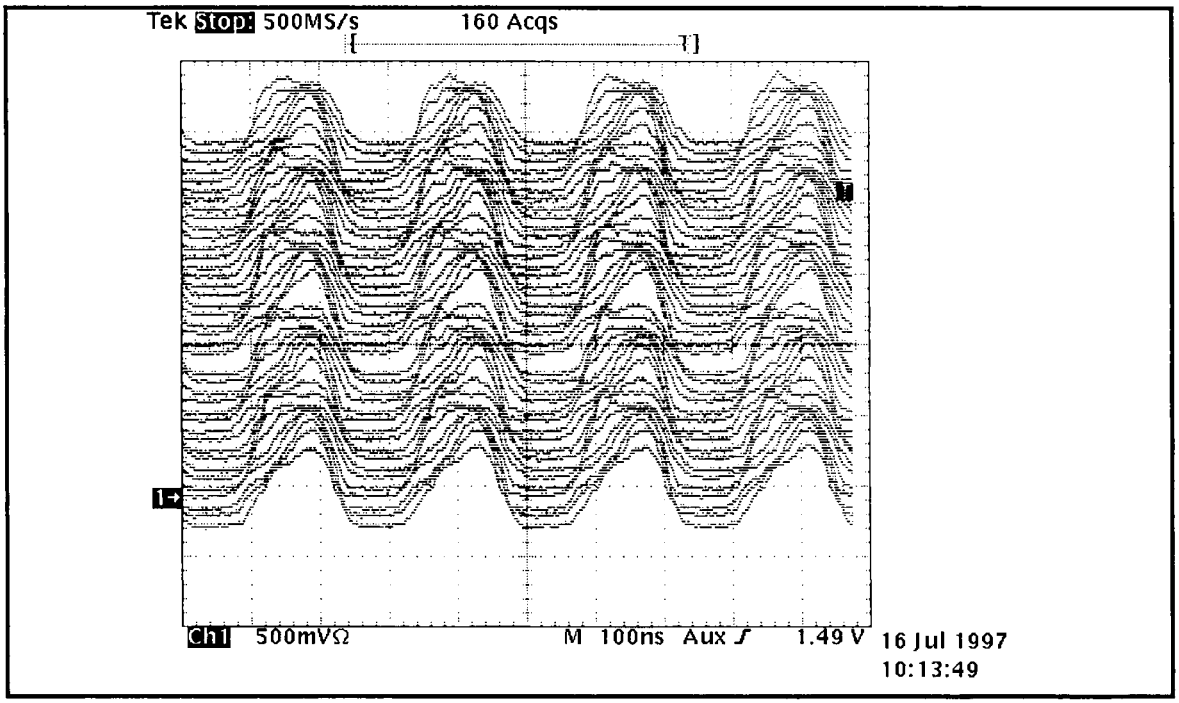

Figure 3.22 Beam signal scanned each 10 revolutions starting from C247 (bottom trace) and lasting 500 μs for φ_2 sliding from 0° to 180°

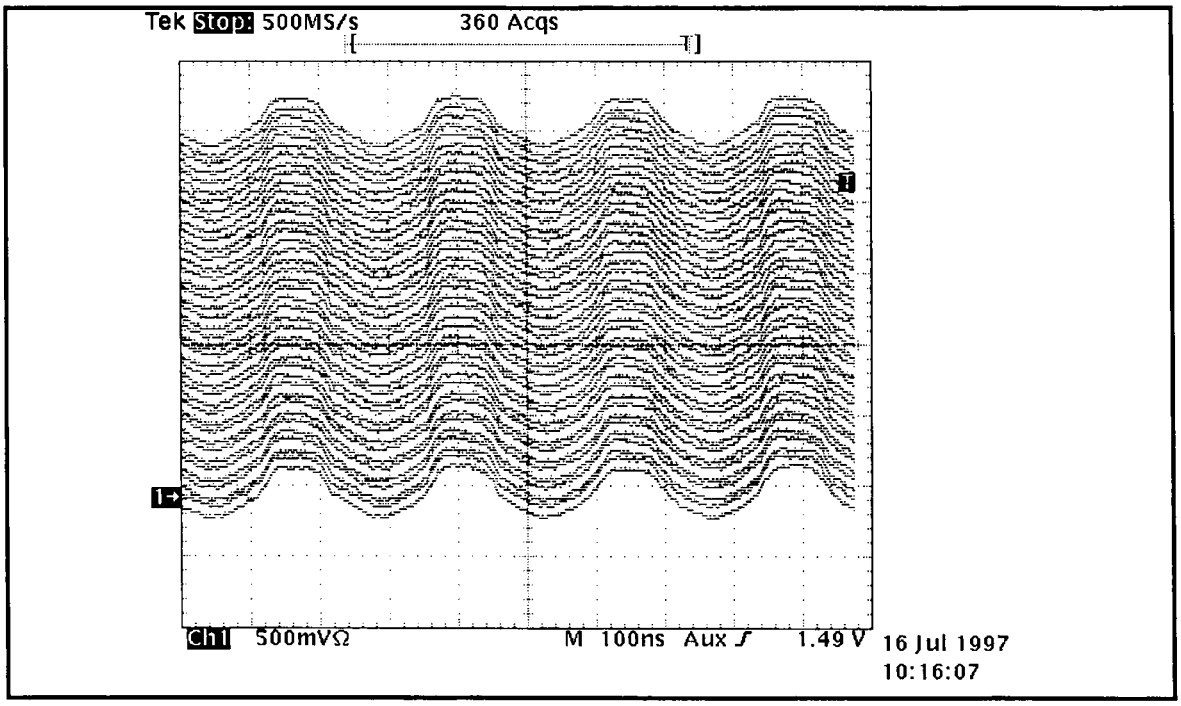

Figure 3.23 Beam signal scanned each 10 revolutions starting from C300 (bottom trace) and lasting 500 μs for φ_2 sliding from 0° to 180°

3.5 Voltage dependence

We now investigate the stability as function of the voltage ratio between the two RF systems and as a function of their relative phasing. To do this, the voltage ratio is set and then the phase is slowly ramped from 0 to 180 starting at C171 and finishing at C271.

Strictly speaking, when the voltage is changed, one expects the synchrotron frequency to change; and so monitoring the amplitude of a signal at 9.7 kHz, does not necessarily give a true indication of the "mode activity". Consequently, the first point of reference must be the beam phase loop signal given as "Trace 2" on the oscillograms.

3.5.1 V2 is 30% of V1

The 2nd harmonic is 30% of the fundamental. (Previously we had 2nd harmonic 50% of fundamental.) The beam is stable when φ=0, and unstable when φ=180, as shown in Fig.3.24. When a phase ramp is introduced, as in Fig.3.25 then the instability starts at C243 when the phasing is 160 degrees, Fig.3.26

Figures 3.27 to 3.30 show the corresponding beam evolution (mountain range plots) from stability at C241 through instability (C243) to saturation C295; for case of C16=3kV.

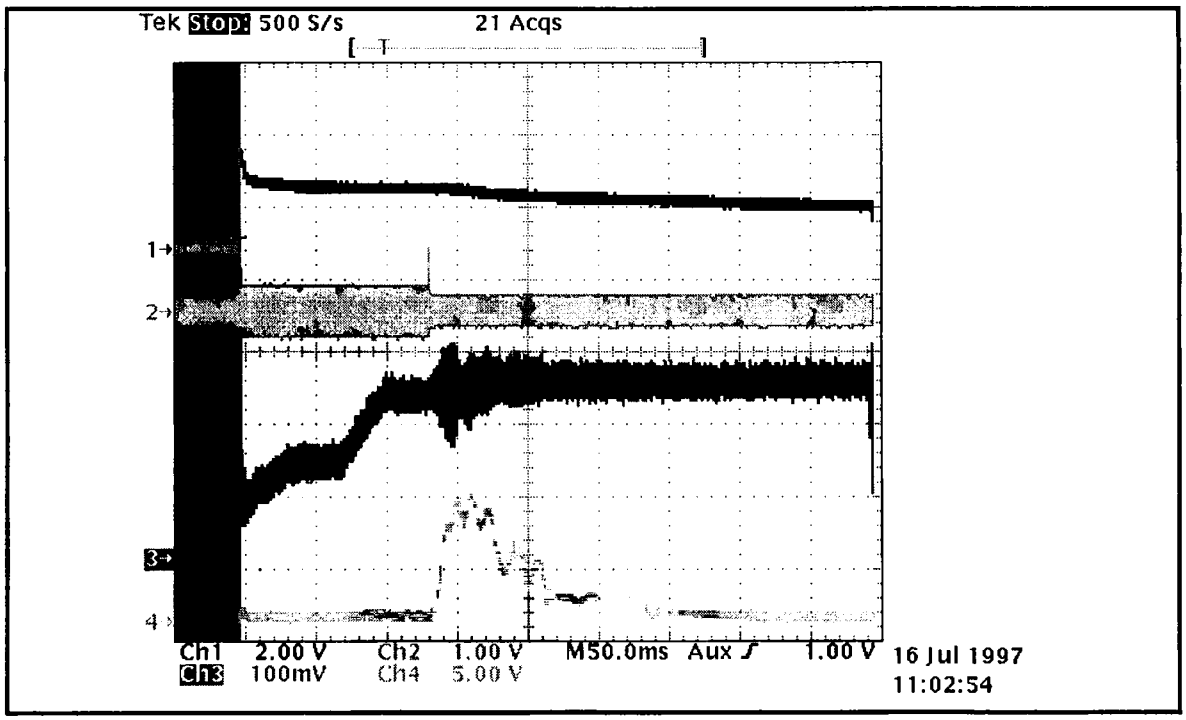

Figure 3.24 Same as fig 3.2 with $V_{rf\,2}$ = 3 kV (30% of $V_{rf\,1}$), φ_2 = 180° (flat bunch)

Trace 1: DC beam current 4 E12 p/V
Trace 2: rf reference beam to gap switching (gap = low amplitude signal)
Trace 3: First harmonic phase error (beam to cavity) measurement (= $\Delta\Phi$)
Trace 4: m = 3, n = 0 mode measured at 3 f_S = 9.7 kHz.

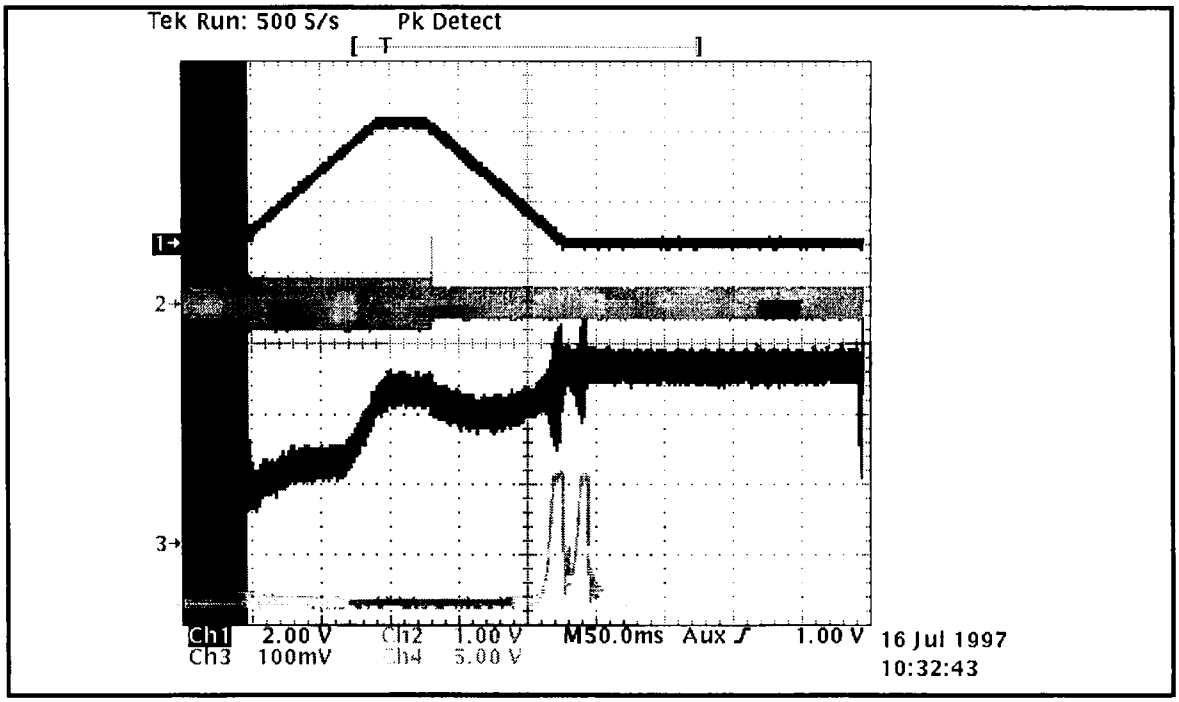

Figure 3.25 Same picture as 3.18 with 2nd harmonic at 3 kV (30% of h1),

Trace 1: 1st to 2nd harmonic phase (bottom = 180, top = 0° (short bunch)
Trace 2: rf reference beam to gap switching (gap = low amplitude signal)
Trace 3: First harmonic phase error (beam to cavity) measurement (= $\Delta\Phi$).
Trace 4: m = 3, n = 0 mode measured at 3 f_S = 9.7 kHz

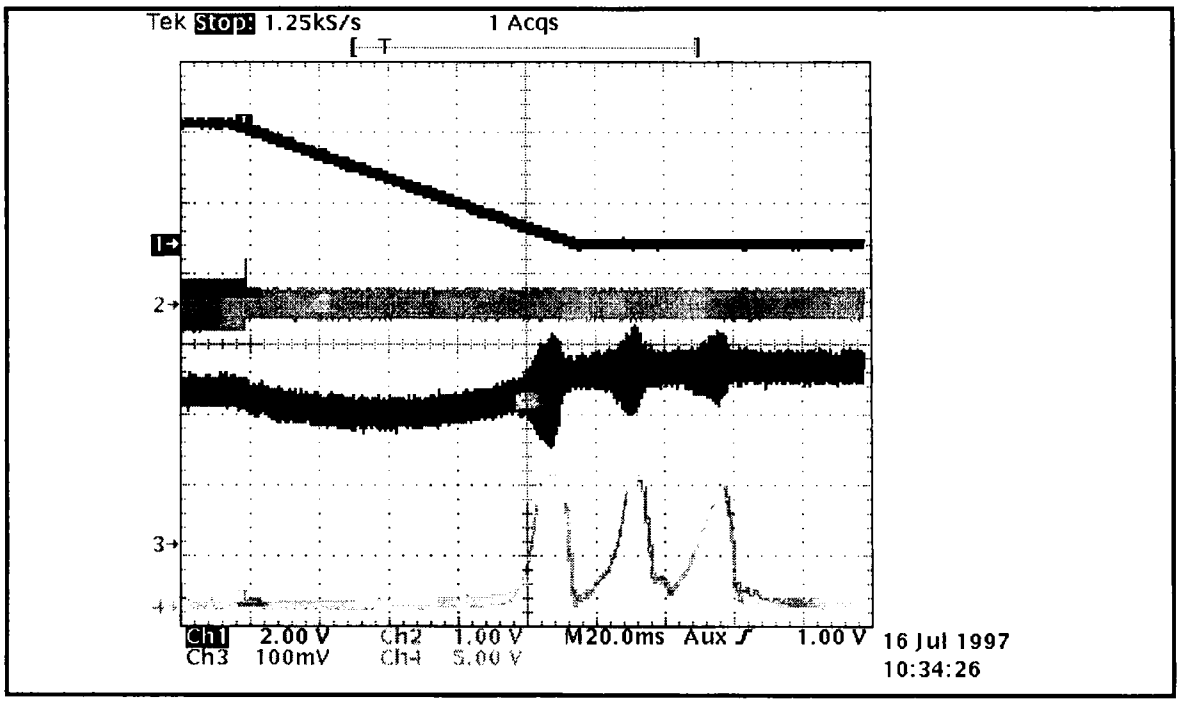

Figure 3.26 Zoom of figure 3.25 showing instability starts circa C245.

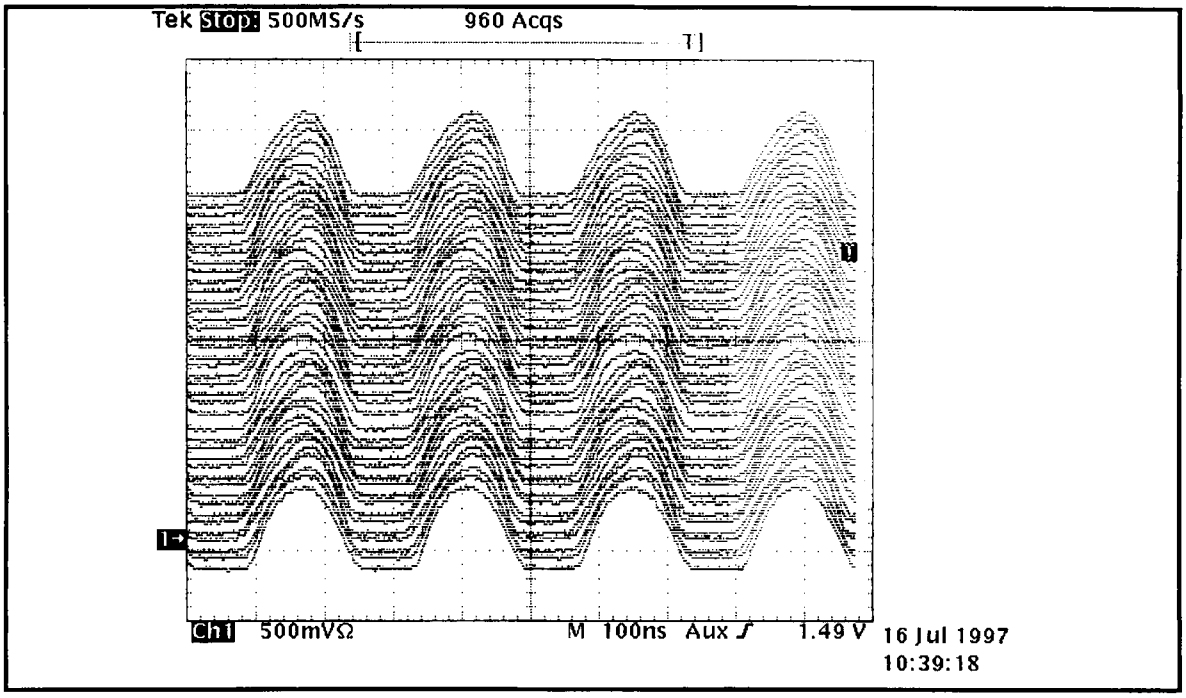

Figure 3.27 Beam signal scanned each 10 revolutions starting from C241 (bottom trace) and lasting 500 μs for φ_2 sliding from 0° to 180° with $V_{rf2} = 3$ kV.

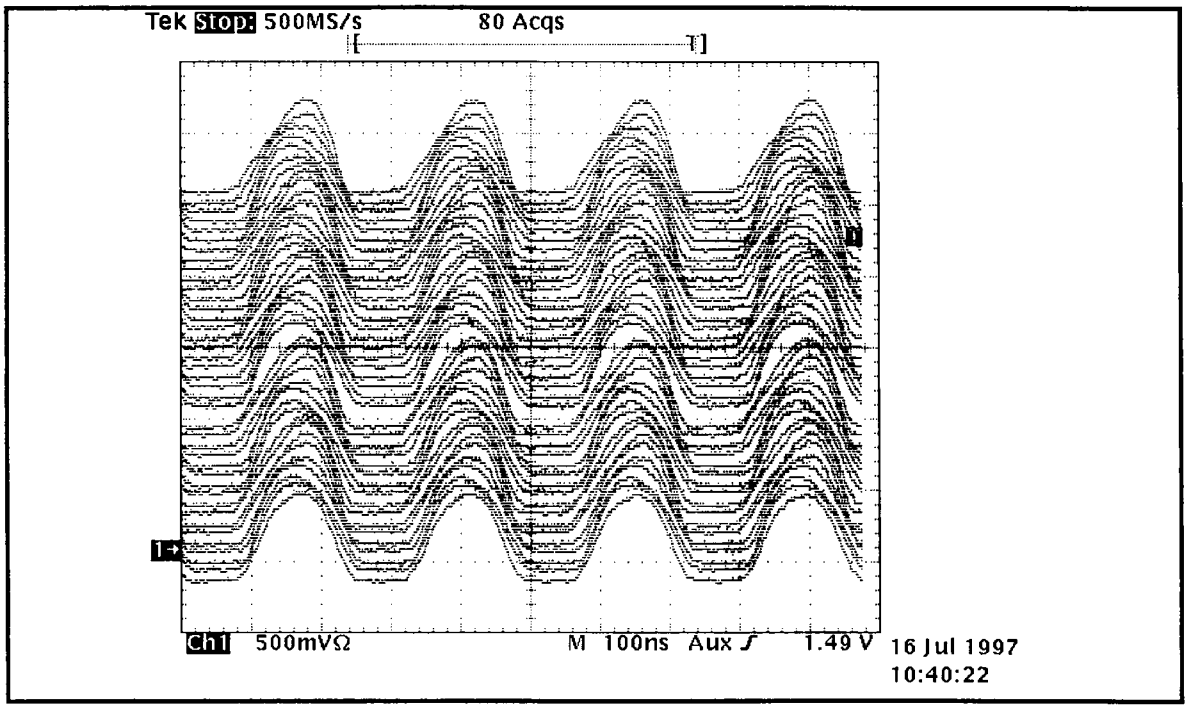

Figure 3.28 Beam signal scanned each 10 revolutions starting from C243 (bottom trace) and lasting 500 μs for φ_2 sliding from 0° to 180° with $V_{rf2} = 3$ kV.

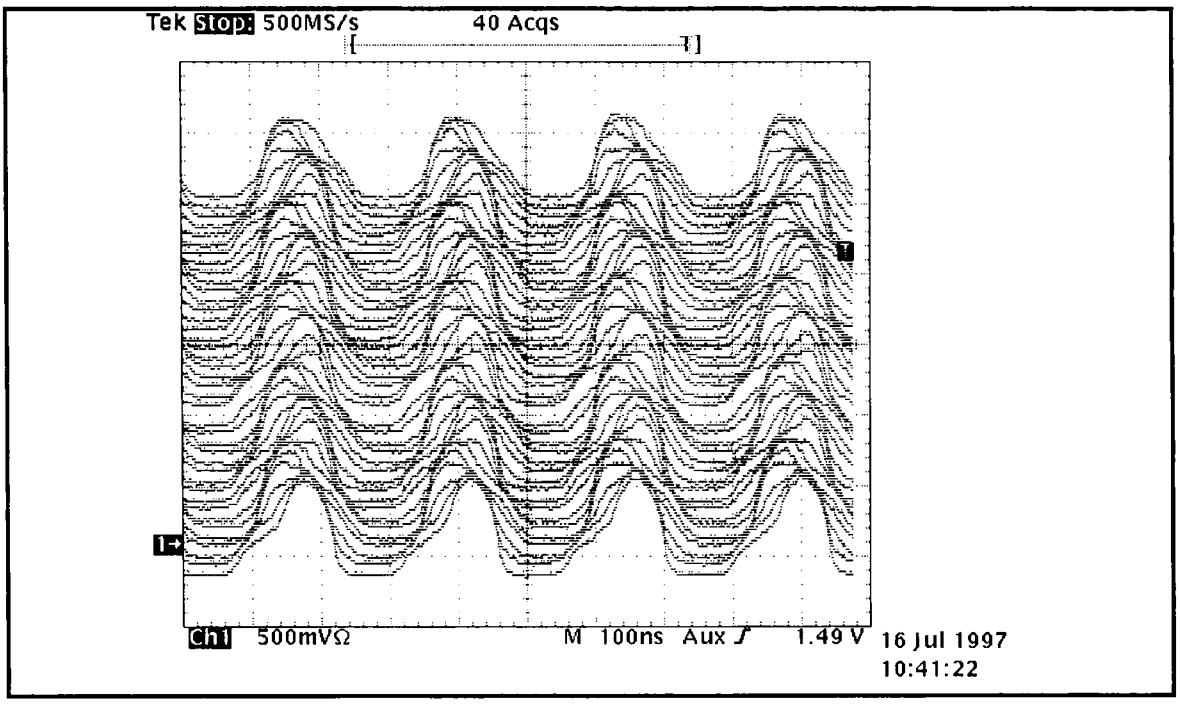

Figure 3.29 Beam signal scanned each 10 revolutions starting from C255 (bottom trace) and lasting 500 μs for φ_2 sliding from 0° to 180° with $V_{rf\,2}$ = 3 kV. The sextupole mode is quite violent at this time.

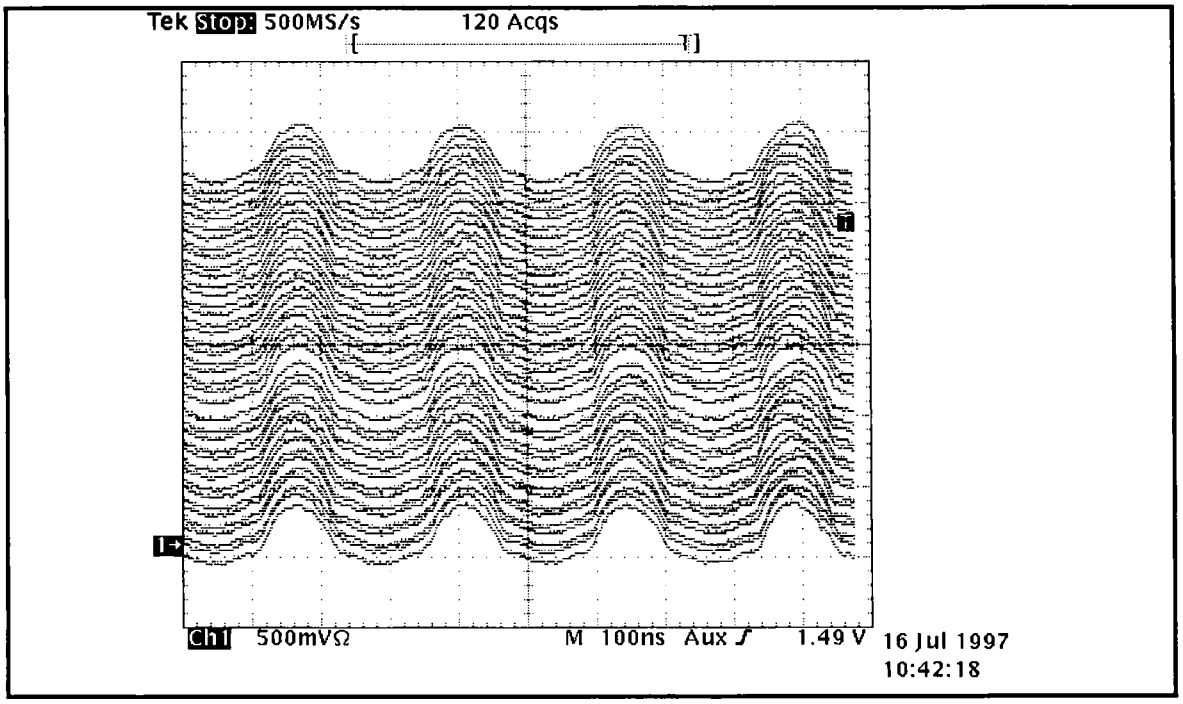

Figure 3.30 Beam signal scanned each 10 revolutions starting from C295 (bottom trace) and lasting 500 μs for φ_2 sliding from 0° to 180° with $V_{rf\,2}$ = 3 kV. Note the tails which accompany self-stabilization of the bunch oscillation.

3.5.2 V2 is 20% of V1

The 2nd harmonic is 20% of the fundamental. The beam is stable when φ_2 =0, and unstable when φ_2 =180, as shown in Fig.3.31. When a phase ramp is introduced, as in Fig.3.32, then the instability starts after C269 when the phasing is 180 degrees. Fig.3.33 shows the frequency to be approx 9.6 kHz

Figures 3.34 to 3.36 show the corresponding beam evolution (mountain range plots) from almost stable at C270 through to full blown instability at C435). For case of C16=2kV.

The basic conclusion is that growth rate is much lower or even non existent when the 2nd harmonic voltage is less than 20% of the fundamental. Indeed, test with V2=25% of the fundamental show very slow growth of the instability; though commutation is at C170, the sextupolar oscillations are still quite mild at C395.

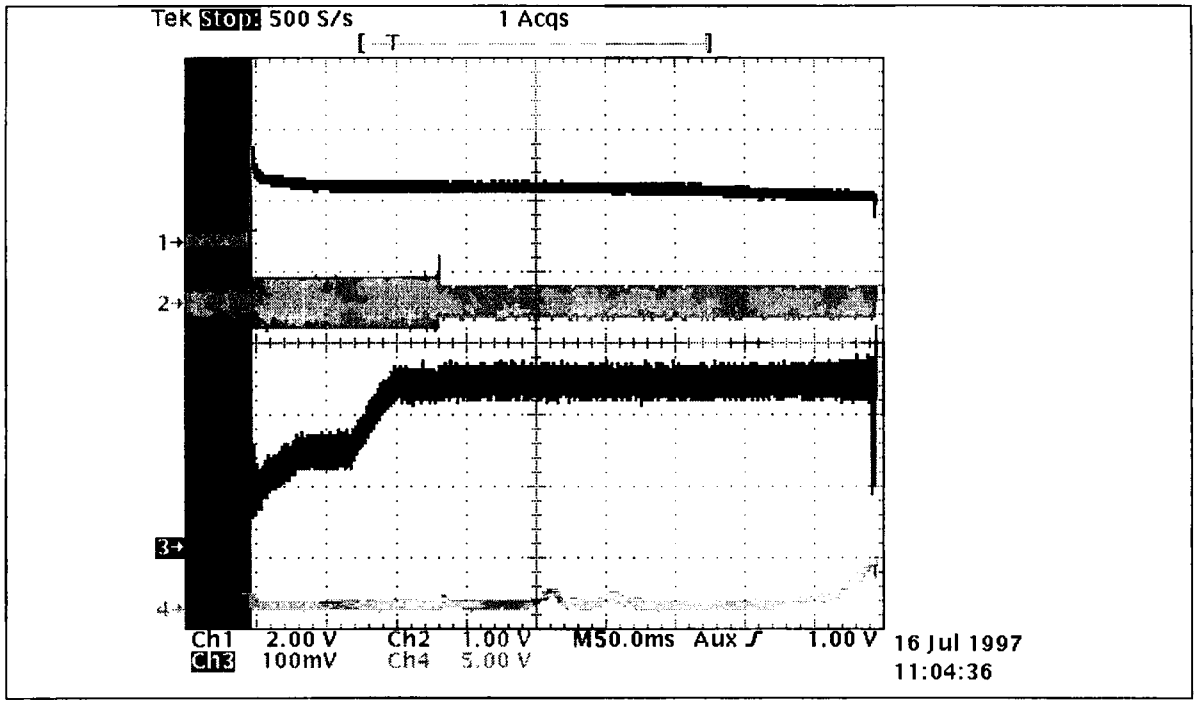

Figure 3.31 Same as Fig 3.2 with V_{rf2} = 2 kV (20% of V_{rf1}), φ_2 = 180° (flat bunch)

Trace 1: DC beam current 4 E12 p/V
Trace 2: rf reference beam to gap switching (gap = low amplitude signal)
Trace 3: First harmonic phase error (beam to cavity) measurement (= $\Delta\Phi$).
Trace 4: m = 3, n = 0 mode measured at 3 f_S = 9.7 kHz

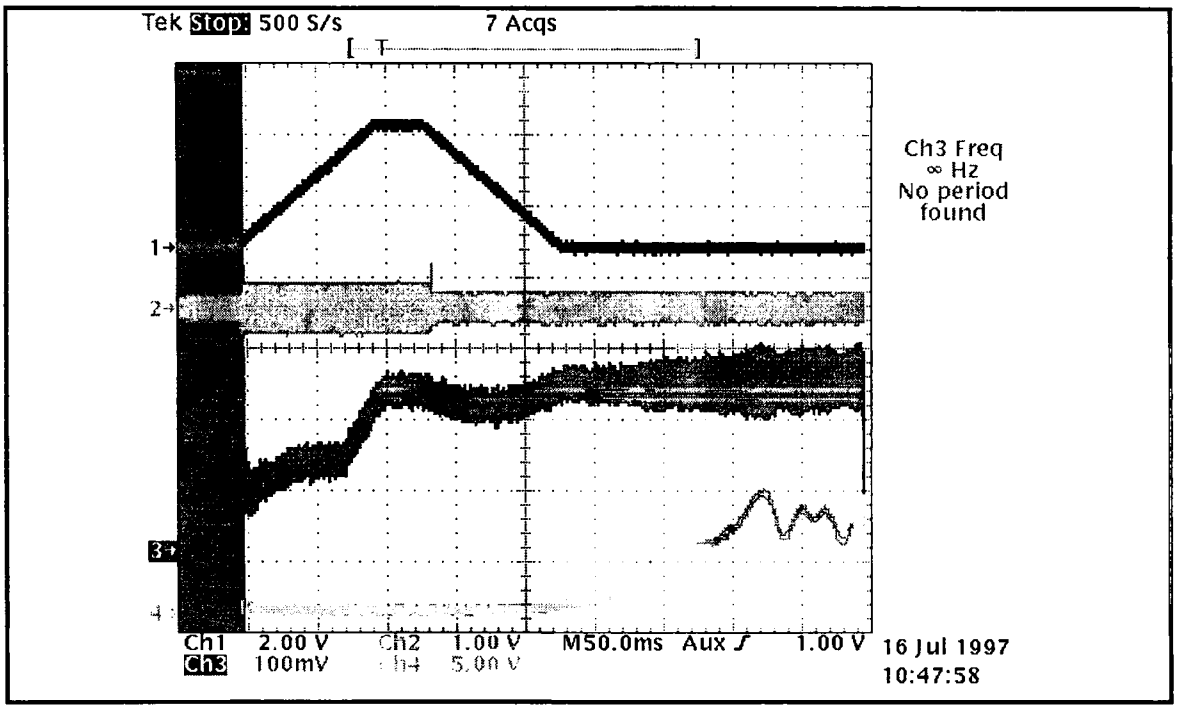

Figure 3.32 Same picture as 3.18 with 2nd harmonic at 2 kV (20% of h1),

Trace 1: 1st to 2nd harmonic phase (bottom = 180, top = 0° (short bunch)
Trace 2: rf reference beam to gap switching (gap = low amplitude signal)
Trace 3: First harmonic phase error (beam to cavity) measurement (= $\Delta\Phi$).
Trace 4: m = 3, n = 0 mode measured at 3 f_S = 9.7 kHz

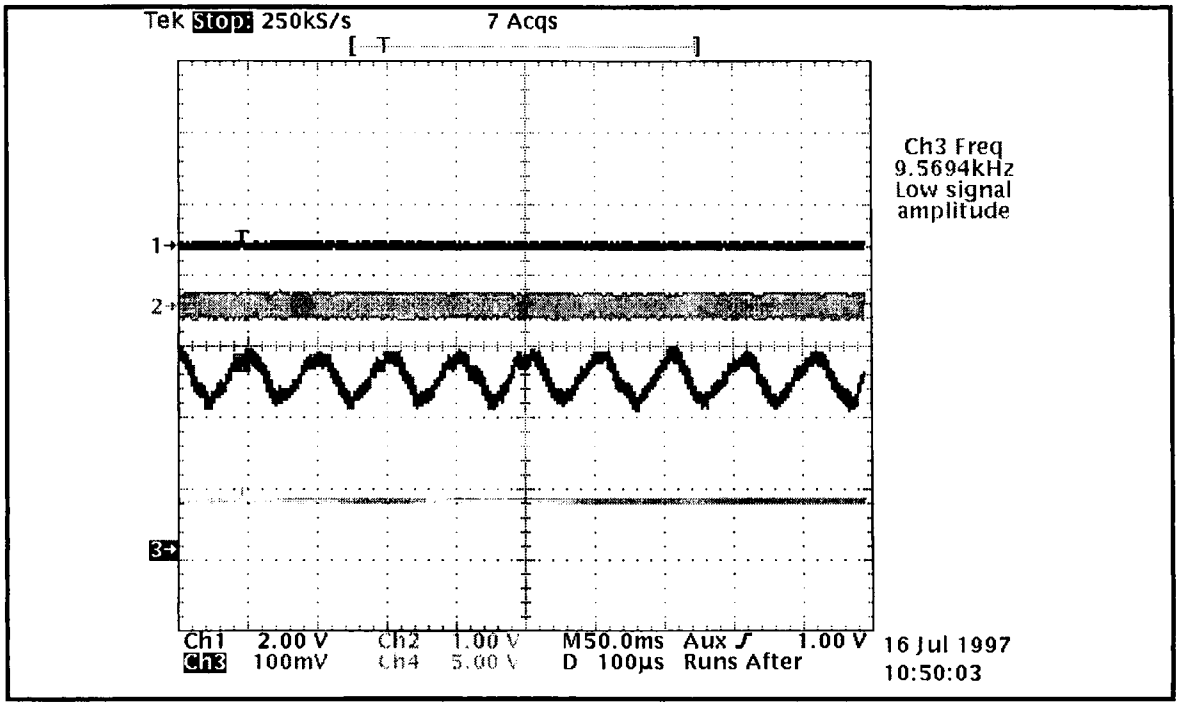

Figure 3.33 Zoom of figure 3.32

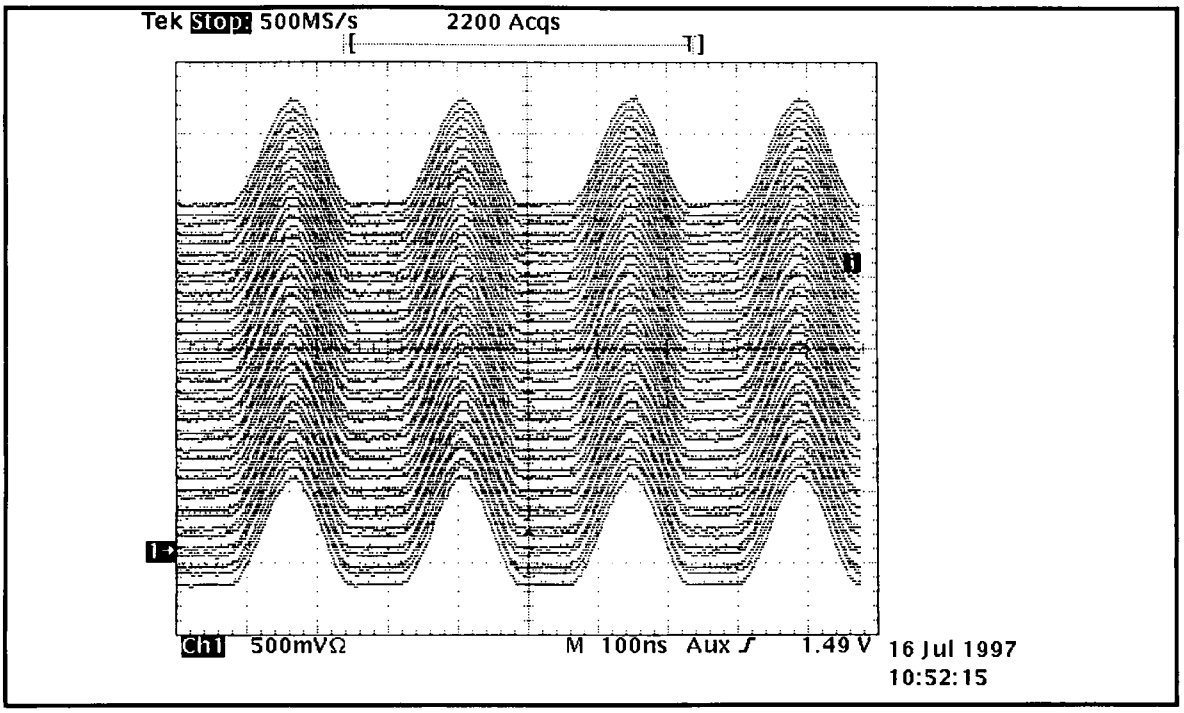

Figure 3.34 Beam signal scanned each 10 revolutions starting from C169 (bottom trace) and lasting 500 μs for φ_2 sliding from 0° to 180° with $V_{rf\,2}$ = 2 kV

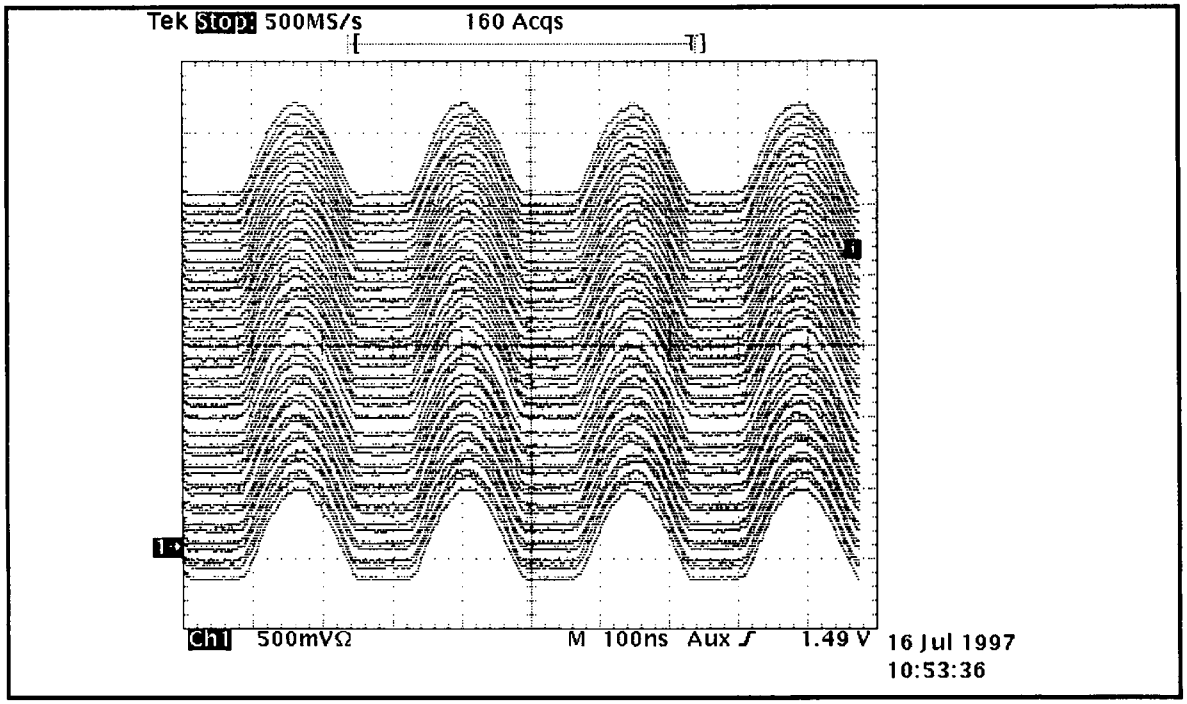

Figure 3.35 Beam signal scanned each 10 revolutions starting from C270 (bottom trace) and lasting 500 μs for φ_2 sliding from 0° to 180° with $V_{rf\,2}$ = 2 kV. Because of the adiabatic sliding, the bunch shape changes, but there is not yet any instability.

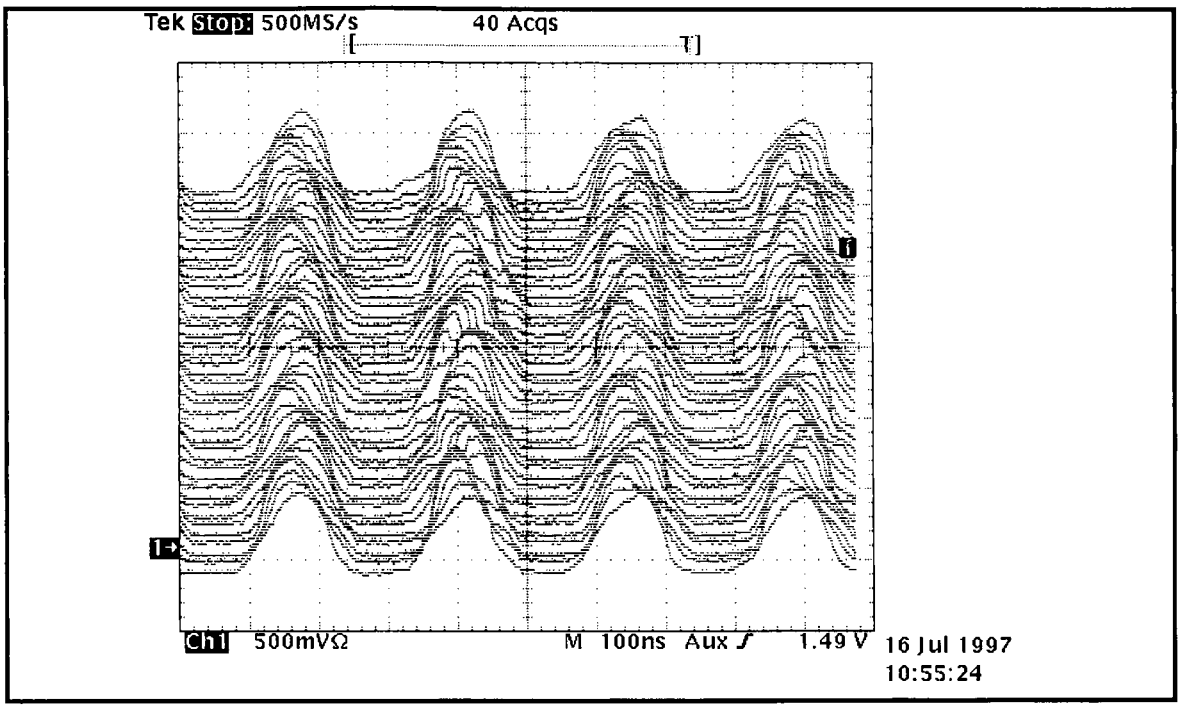

Figure 3.36 Beam signal scanned each 10 revolutions starting from C435 (bottom trace) and lasting 500 μs for φ_2 sliding from 0° to 180° with $V_{rf\,2}$ = 2 kV. Instability starts when ϕ_2 reaches 180^0.

N.B. If you compare Fig.3.32 with 3.25 or 3.18, then you conclude the growth rate is slower with V_2= 20% of V_1.

4 Tests with Digital Beam Control

After 4:30 p.m. Wednesday 16th July, we began tests with an all digital beam control. In particular, the second harmonic corrector was made proportional with an ideal gain of 10(from PLA)×4(DLP gain)=40.

4.1 Comparison with standard cases

Apart from the digital control, we reproduced the standard case of section 3.1, figure 3.2, as a consistency and calibration check with previous work. Figure 4.1 shows the oscillogram traces and a clear signal of sextupolar instability in the mode analyser trace on channel #4. Commutation is at C170. Figure 4.2 shows the sextupolar oscillation in `full swing' and Figure 4.2 shows the self-stabilisation by the formation of tails. Initially the bunches are 270 degrees long. After stabilisation, they grow to 305 degrees long and with a discontinuity in the slope at approximately ±90°.

N.B. If you compare Fig.4.1 with Fig.3.2, then you conclude the growth rate is slower with digital control than with analogue.

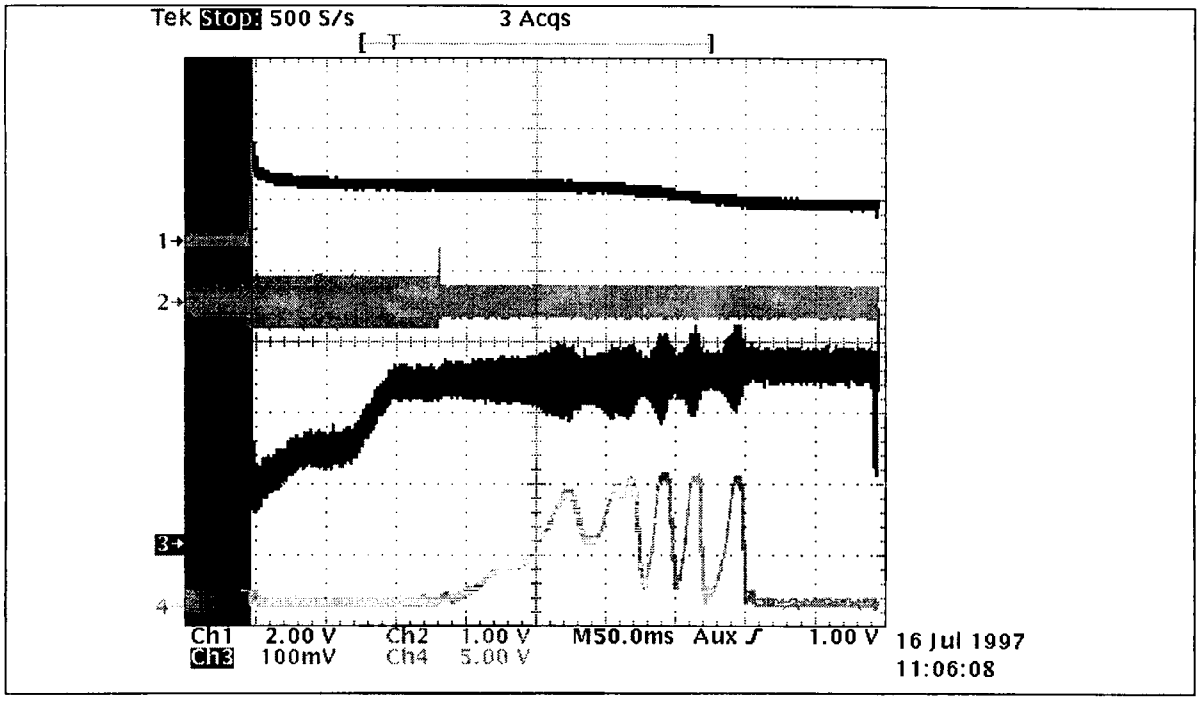

Figure 4.1 Oscillogram traces for case of digital beam control for cavities anti-phased.

Trace 1: beam current 4E12 p/V
Trace 2: beam to gap commutation at C170.
Trace 3: beam phase loop signal.
Trace 4: m=3, n=0 mode analyser signal at 3 f_s=9.7 kHz.

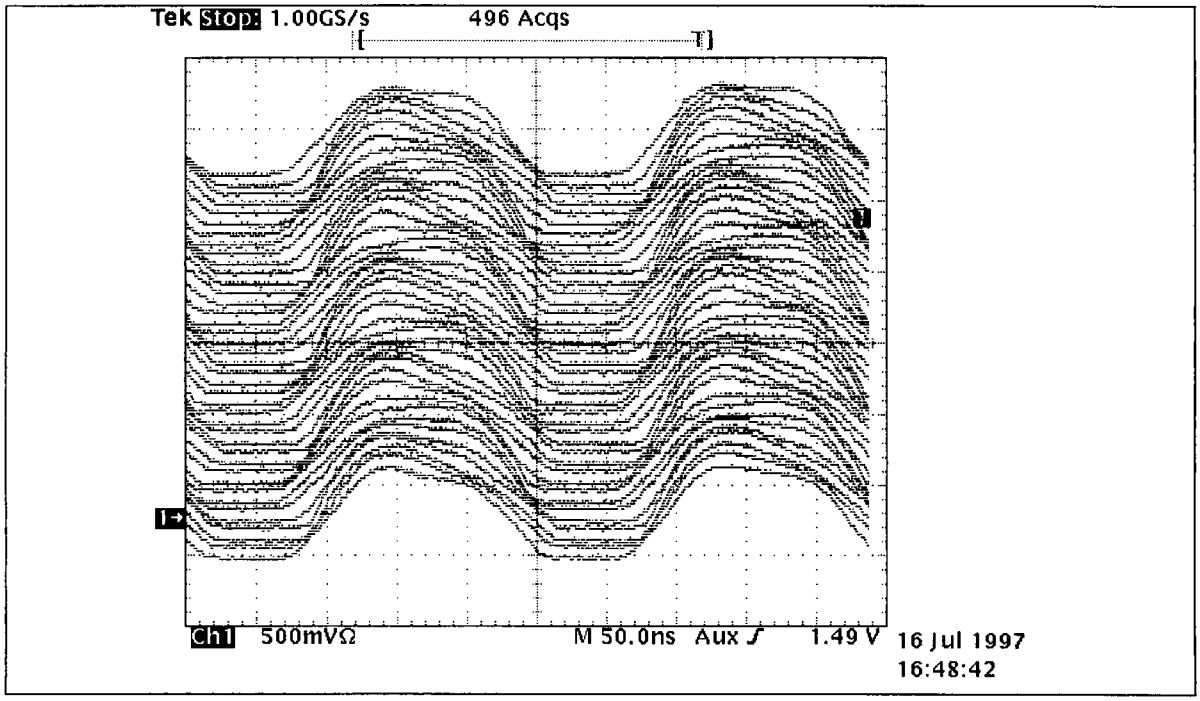

Figure 4.2 Mountain range plot for long bunch mode with digital control. Scan is triggered at C174 (bottom) and duration is 500 μs, traces each 10 revolutions.

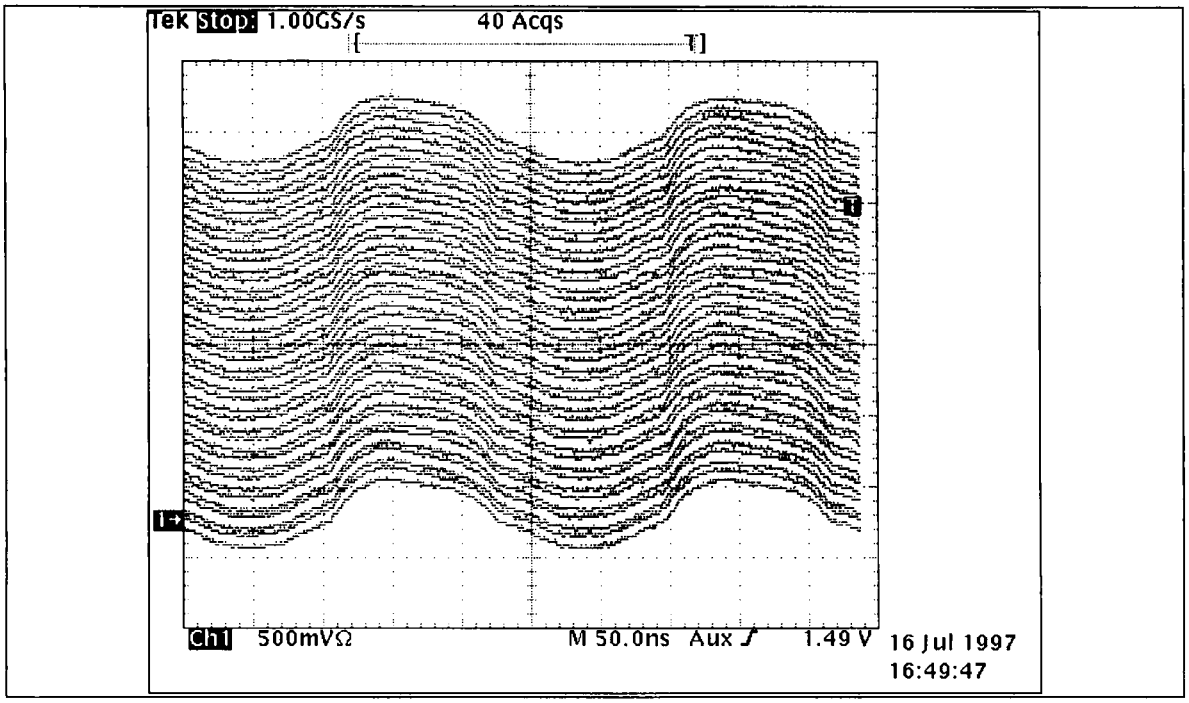

Figure 4.3 Mountain range display of bunch shapes. Scan is triggered at C274 and continues for 500 μs. Note formation of tails during self-stabilization.

4.2 Short bunch mode

Again, for comparison with the analogue control, section 3.3 figures 3.15—3.17, we prepared a standard short bunch with the cavities in-phase. As anticipated, there is no instability. Figure 4.4 shows the mode analyzer trace to be completely flat both before and after commutation of the SHC signal from beam to gap. Figure 4.5, the mountain range display, shows the bunches to be completely stable. The bunch length is ±95°.

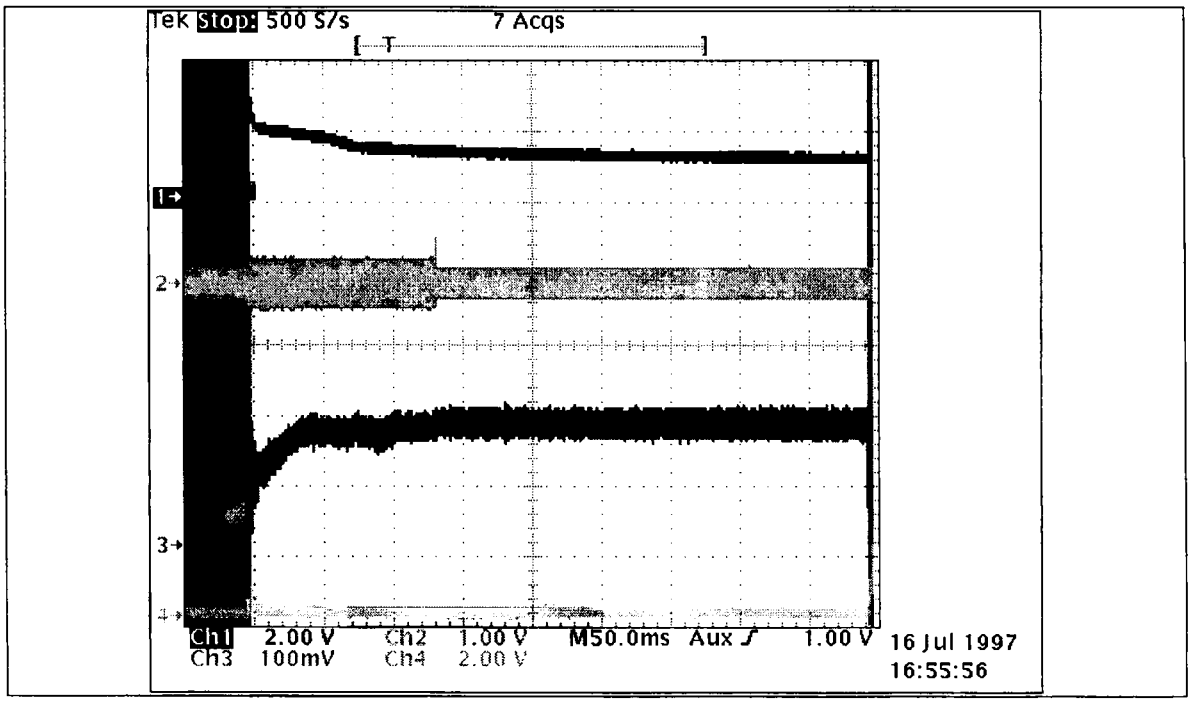

Figure 4.4 Oscillogram traces for short bunch mode with digital SHC control.

Trace 1: beam current 4E12 p/V
Trace 2: commutation signal with switching at C170.
Trace 3: beam phase loop signal
Trace 4: mode analyser signal at 3 f_s = 9.7kHz.

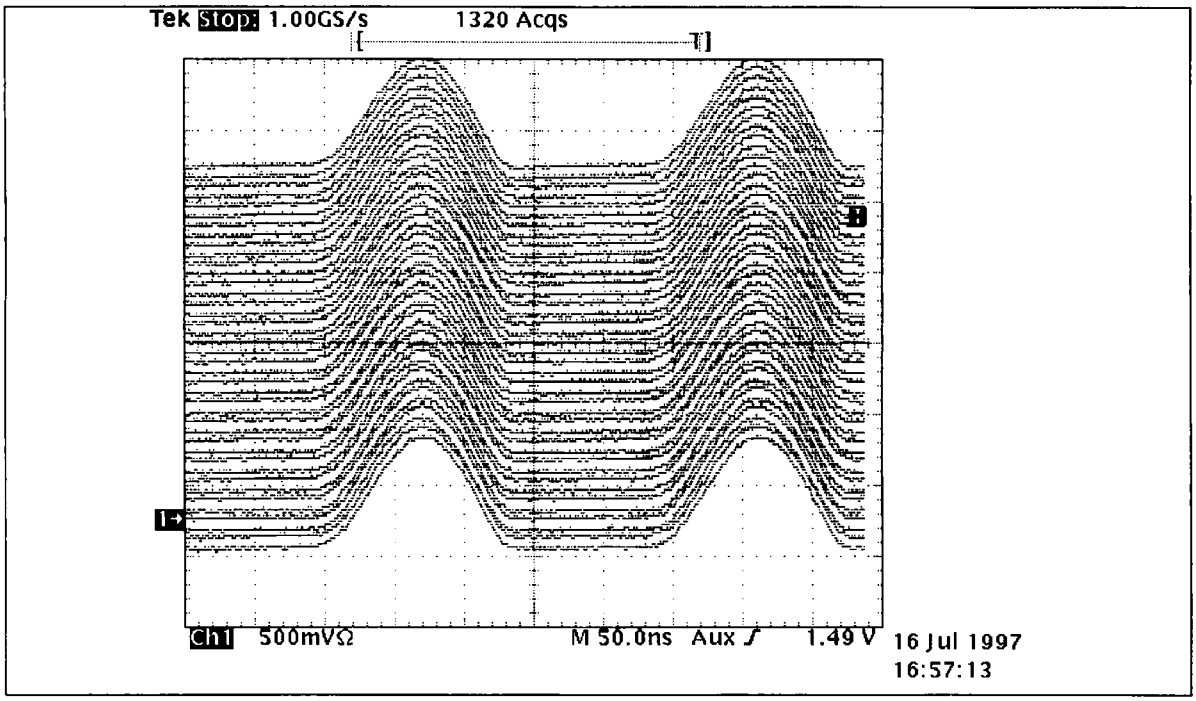

Figure 4.5 Beam signal scanned each 10 revolutions starting from C170 (bottom) and lasting 500 μs for digital control and cavities in-phase (i.e. short bunch mode).

4.3 Dependence on phasing of cavities

Having established that the basic beam behaviour with digital control is the same as for analogue, we now made some more detailed measurements; in particular the dependence on the relative phasing of cavities, φ_2. Figure 4.6 shows an oscillogram when the phase is adiabatically ramped from 0 to 180 degrees (in-phase to anti-phase). The instability starts to appear when $\varphi_2 = 140^\circ$ (similar but not exactly the same as results of section 3.4 –3.5.)

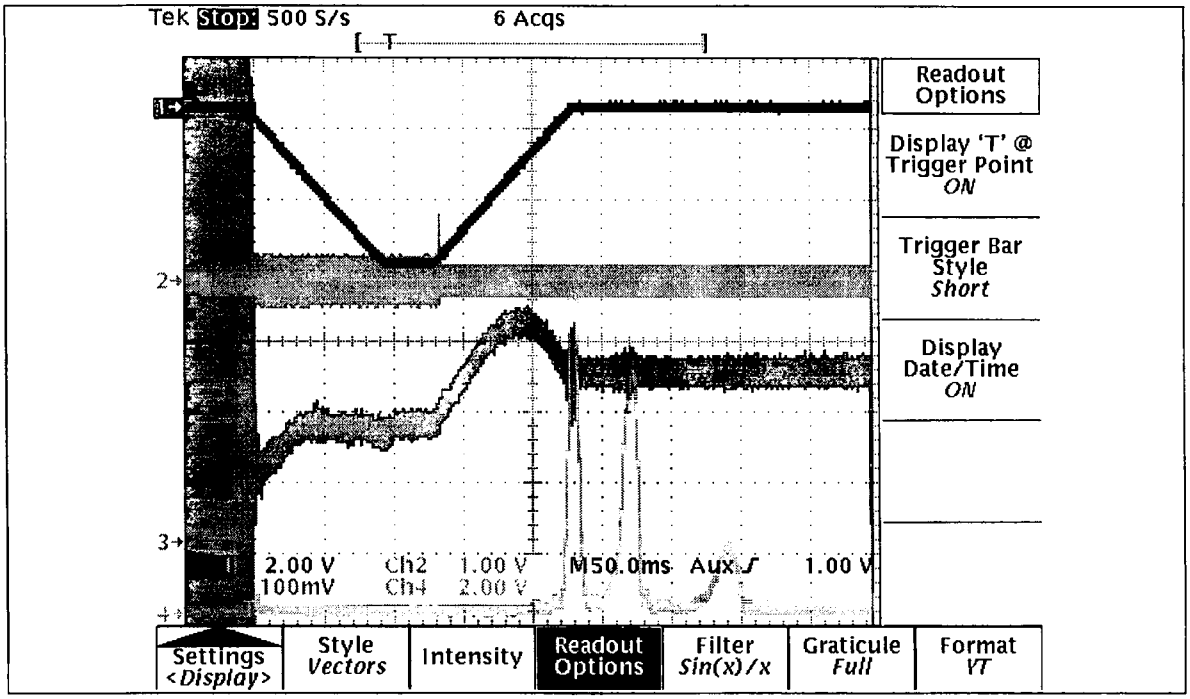

Figure 4.6 Oscillogram for adiabatic phasing ramping with digital beam control.

Trace 1: phase law, φ_2; bottom=0 and top=180 degrees.
Trace 2: commutation signal; high= beam, low= cavity gap
Trace 3: beam phase loop signal
Trace 4; m=3, n=0 mode measured by analyzer at 9.7 kHz.

4.4 Dependence on SHC gain

We now make some qualitative investigation of the instability dependence on SHC gain. Previously, the gain was 40. With a gain=20, there is no discernible difference. With a gain=10, the instability appears, perhaps, to be starting before commutation from the beam to gap. With an SHC gain=5, the instability clearly starts before commutation, as shown in Figure 4.7.

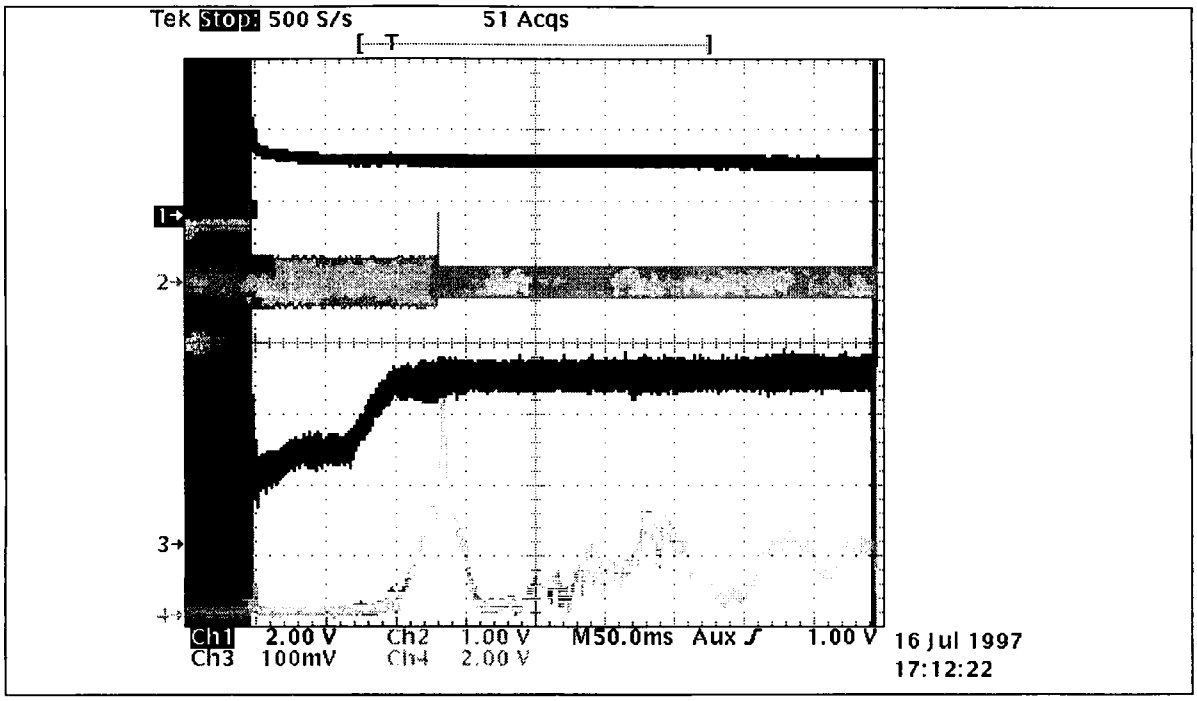

Figure 4.7 Oscillogram traces for SHC gain reduced to 5, showing instability before switching. Traces as for figure 4.6.

5 Very short bunches

We report, now, the results of an MD on Thursday 9th October.

By longitudinal scraping it is possible to make bunches of very small emittance. If these are placed in an RF bucket with the 1st and 2nd harmonic components anti-phased, the result will still be a short bunch.

Working with a 100 MeV FLATCYC (cycle with flat top) and analogue control.

First, with a conventional long bunch (11 injected turns), we optimized the amplitude of the mode analyzer signal at 10.95 kHz. and saw the usual beam instability at switching, Figure 5.1.

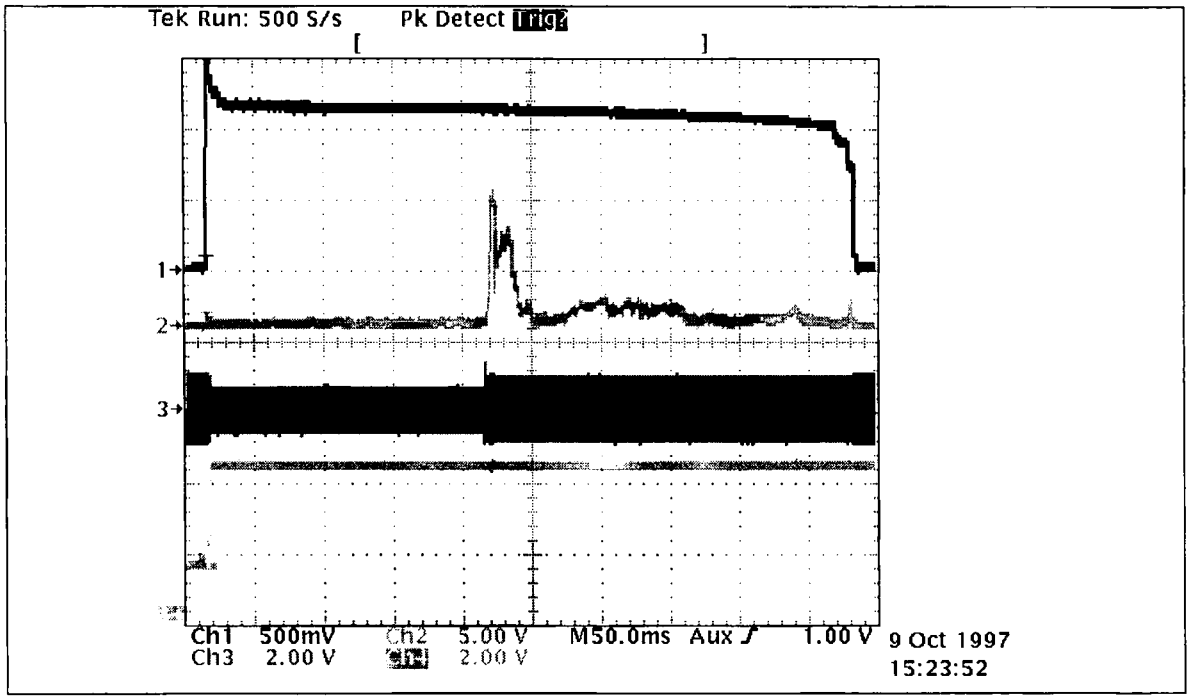

Figure 5.1 Oscillogram for standard beam (long bunches) taken on FLATCYC.

Trace 1: Beam current 4E12 p/V.
Trace 2: m=3 mode analyzer signal at $3f_s$=11 kHz.
Trace 3: commutation signal (low= beam, high= gap).
Trace 4: cavity voltage law.

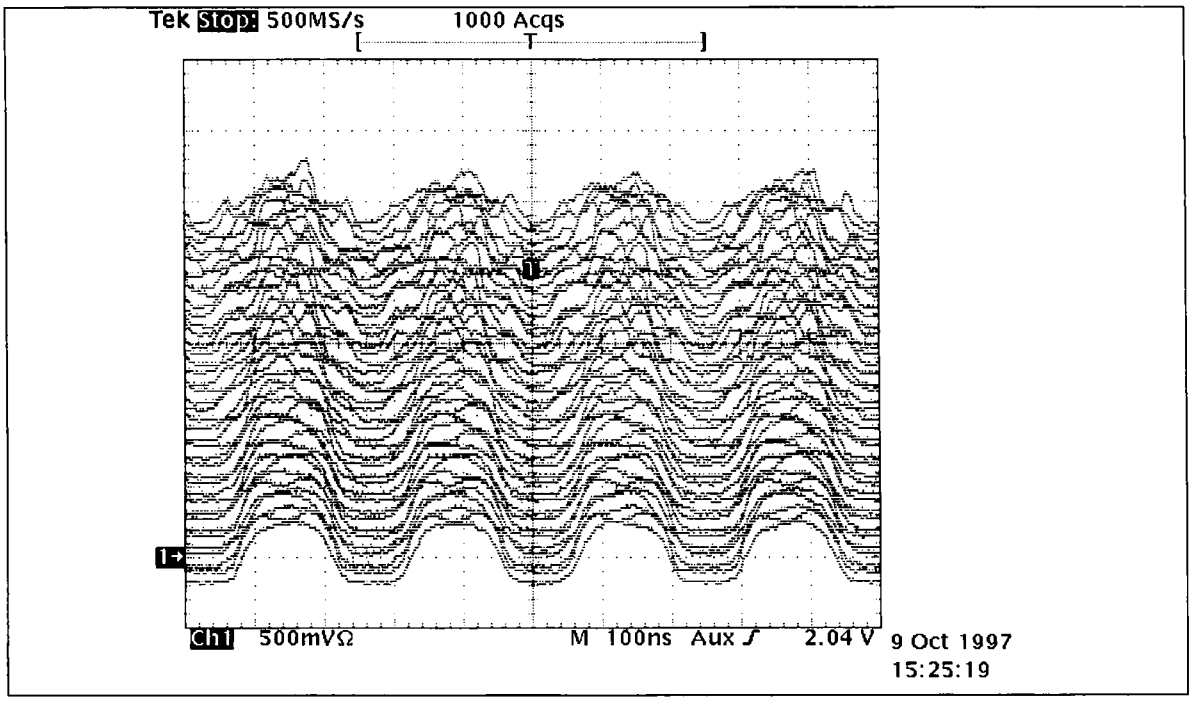

Figure 5.2 The usual long bunch instability. Beam signal is scanned each 100 revolutions starting from C235 (bottom trace) and lasting 5ms.

Then a rectangular cut was made in the voltage program, as shown in Figure 5.3. The h=5 voltage, initially 11.5 kV, was reduced to 1.92 during the magnet ramp, held constant and then returned to 11.5 kV after reaching the flat top; the h=10 component was at all times kept at 50% of the h=5 voltage. This creates a "longitudinal bottle-neck" that results in large losses, but the surviving bunches have a FW bunch length of 100ns or 150° FW.

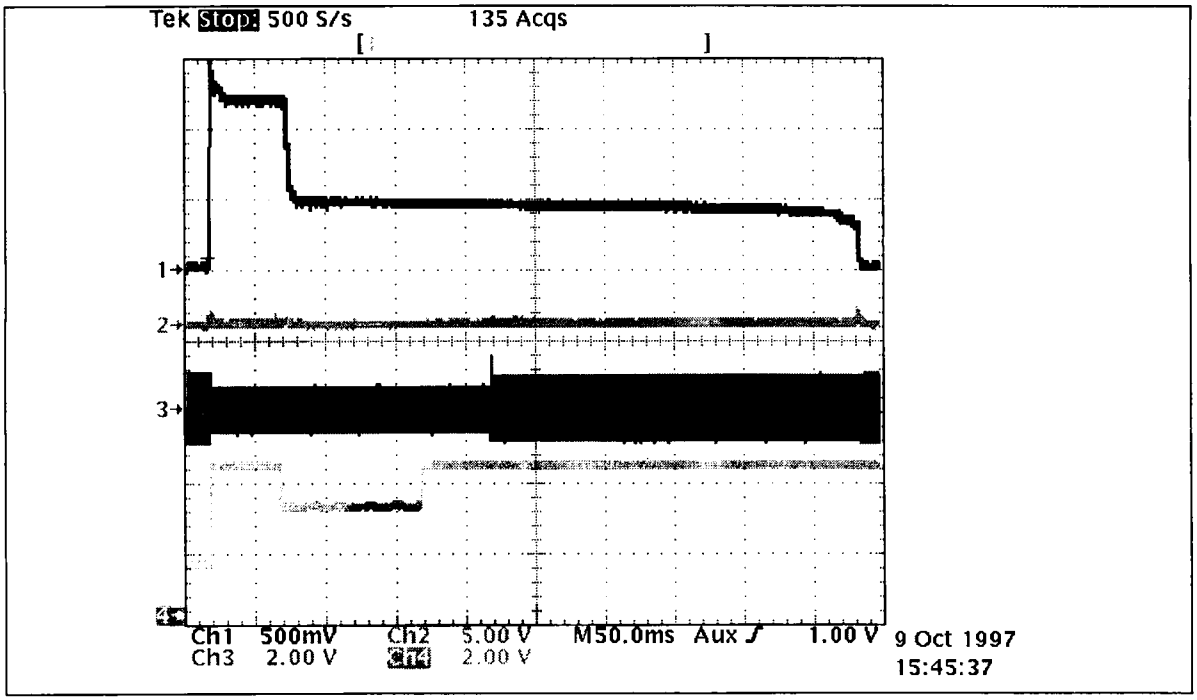

Figure 5.3 Oscillogram trace for longitudinal beam scraping by rectangular cut in voltage law, trace #4. The dramatic beam loss due to scraping during the magnet ramp is trace #1.

Notice in Figure 5.3 that the mode analyzer signal (trace #2) is completely flat, indicating there is no instability at the sextupole frequency. This is confirmed in the mountain range plots of bunch evolution, Figure 5.4 and 5.5 taken 200 ms apart.

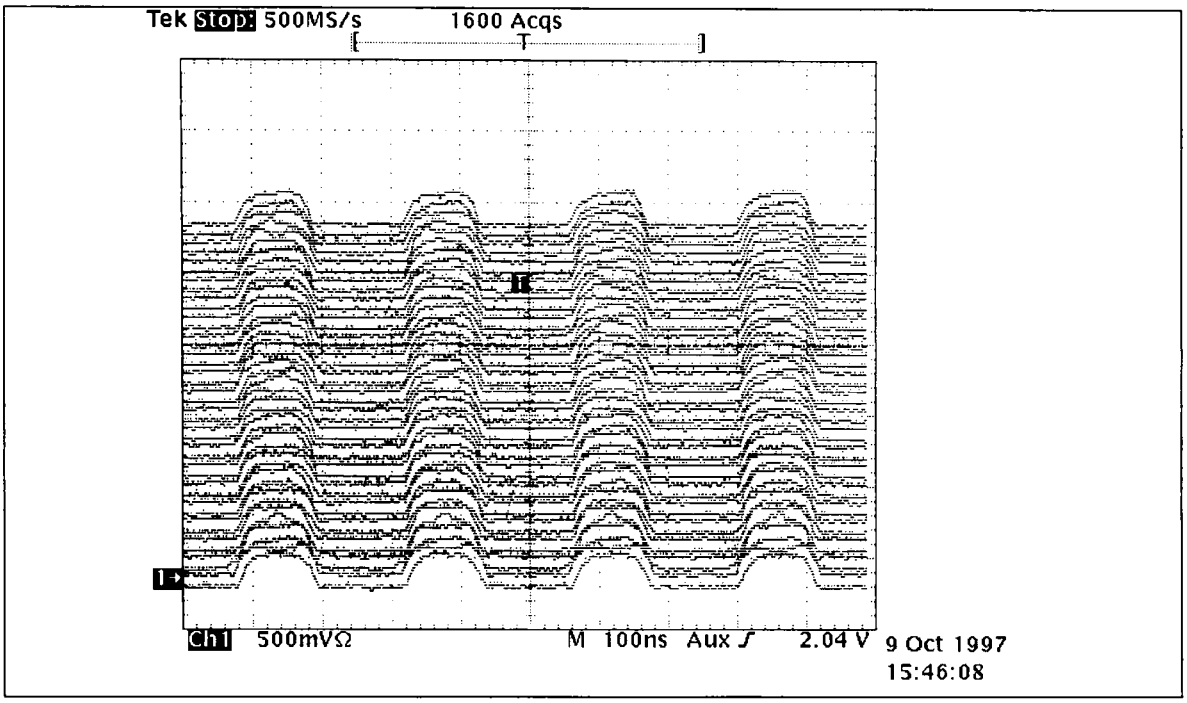

Figure 5.4 Case of longitudinal scraping leads to very short and stable bunches. Beam signal is scanned each 100 revolutions starting from C235 (bottom trace) and lasting 5ms.

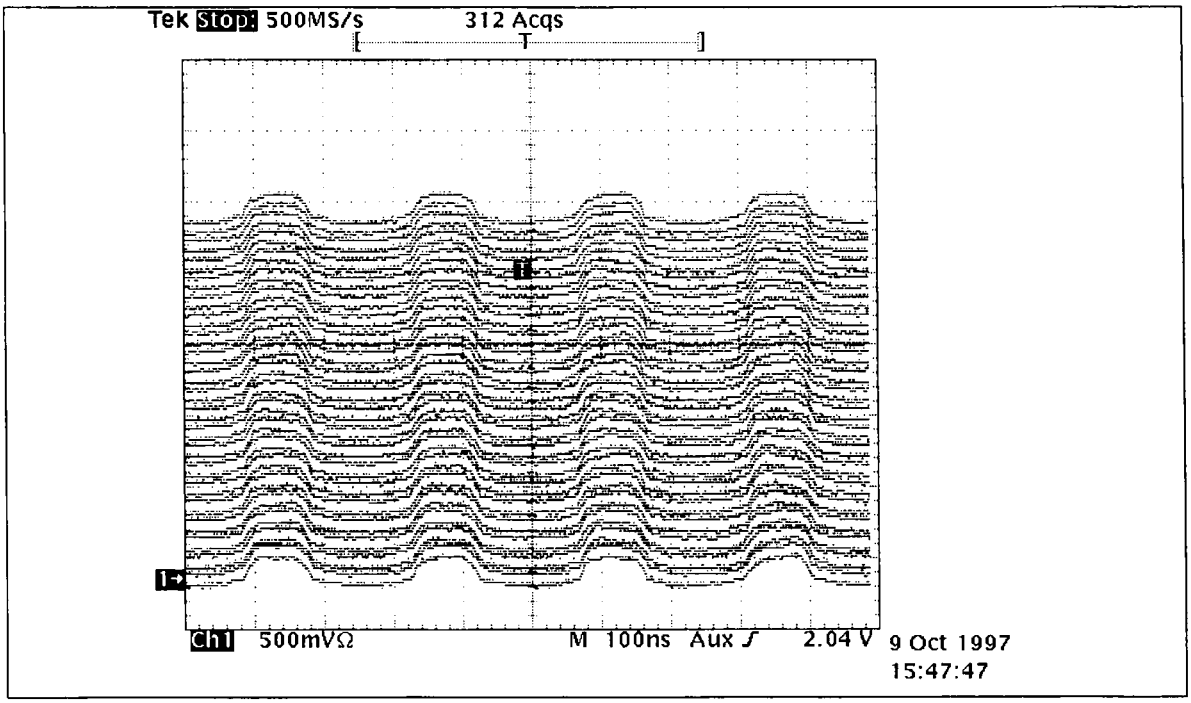

Figure 5.5 Case of longitudinal scraping. Bunches are either stable or have very low growth rate. Beam signal is scanned each 100 revolutions starting from C435 (bottom trace) and lasting 5ms.

5.1 Long bunches of same intensity as the very short

It might be argued that the stability of the short bunches is due to the very low beam current. A long bunch of equivalent intensity to the very short bunches was prepared by

reducing the injected turns from 11 to 2 and not scraping. The equivalent currents can be seen by comparison of Figures and 5.3 and 5.6.

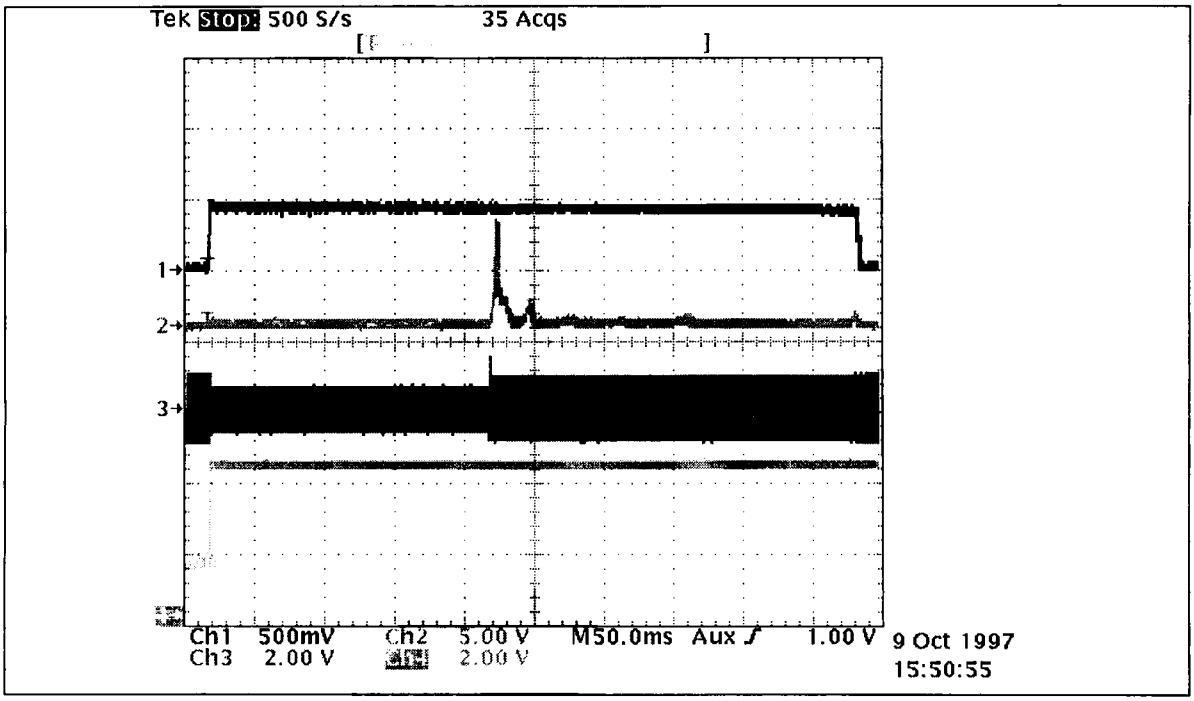

Figure 5.6 Oscillogram for low intensity long bunches. The traces are as for Figure 5.1.

Despite the much reduced beam current (a factor of 5), the long bunches are unstable and develop the usual sextupolar motion. This is shown in the mode analyzer trace, Fig.5.6, and the mountain range plots, Figures 5.7 and 5.8. Figure 5.7 shows the instability at its onset, while Fig. 5.8 shows the eventual self-stabilization by the growth of bunch tails.

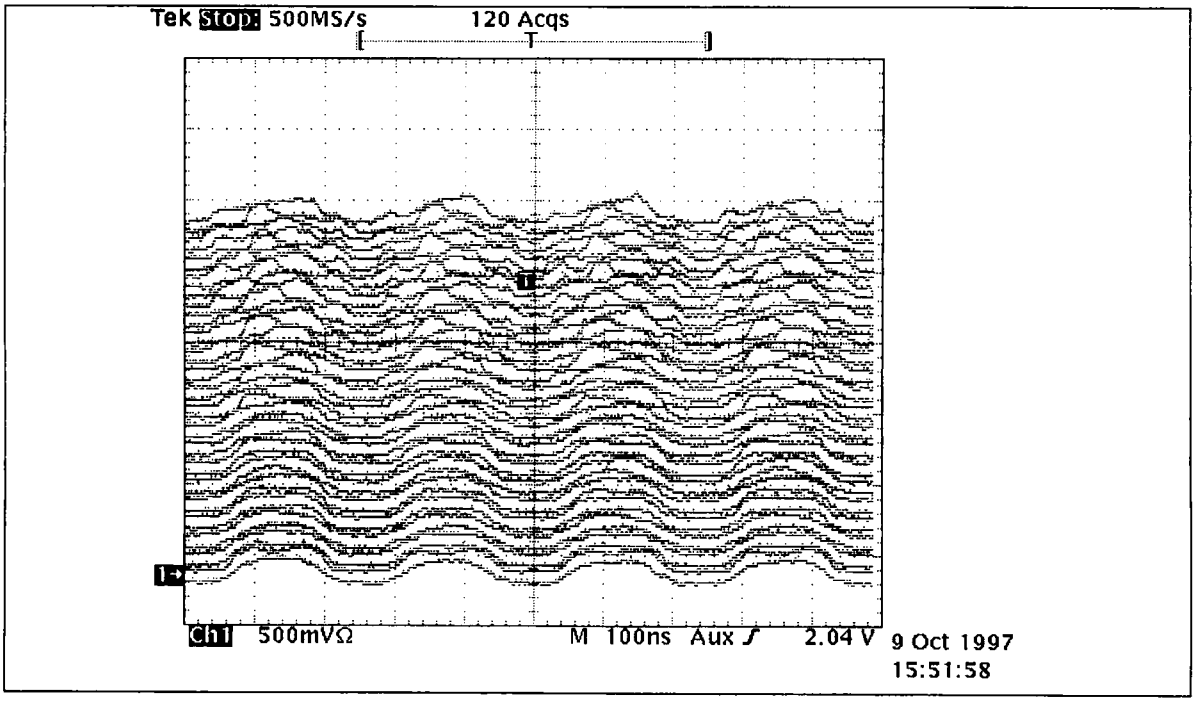

Figure 5.7 Evolution of low intensity long bunches. Beam signal is scanned each 100 revolutions starting from C235 (bottom trace) and lasting 5ms.

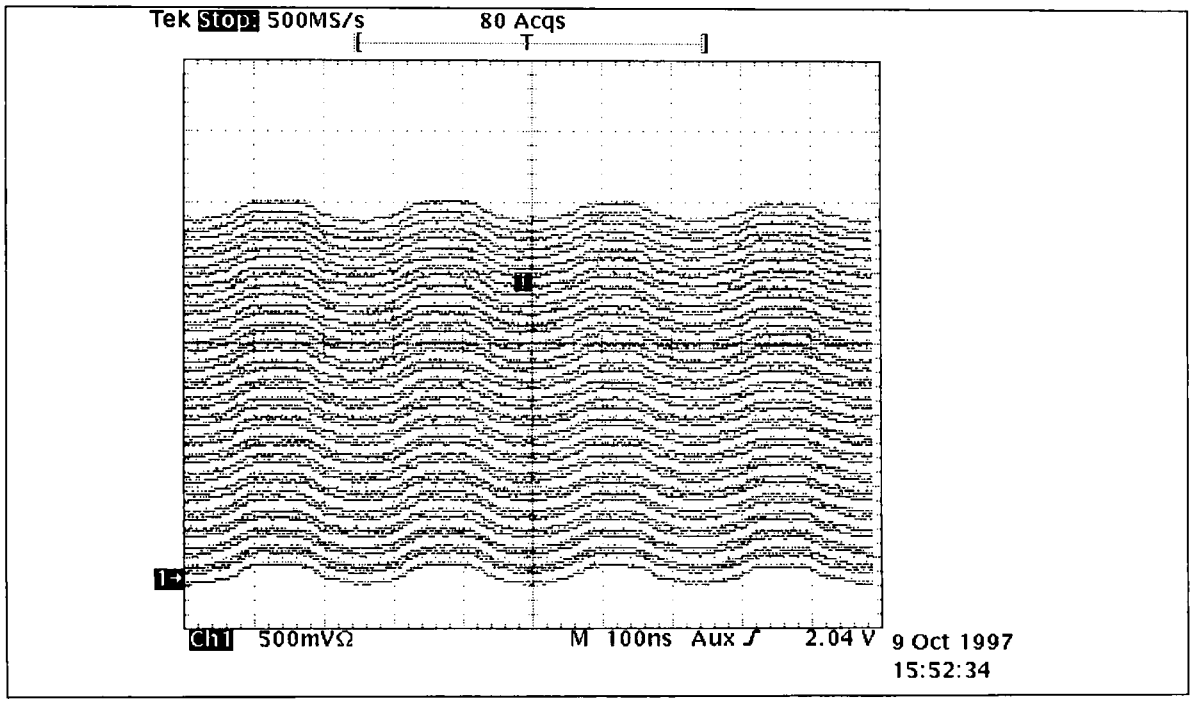

Figure 5.8 Eventual self-stabilization of low intensity long bunches. Beam signal is scanned each 100 revolutions starting from C435 (bottom trace) and lasting 5ms.

As a final experiment, we considered the effect of making the commutation during the magnet field ramp. There was no discernible difference to the results.

6 References

[1] **A Second harmonic RF System with feedback-reduced gap impedance for accelerating flat-topped bunches in the PS Booster,** Baillod, Magnani, Nassibian, Pedersen & Weissflog; IEEE Trans. Nucl. Sci., Vol. NS-20, No.4, p 3449 (1983)

[2] **Electronics for the longitudinal active damping system for the CERN PS Booster,** B. Kriegbaum, F. Pedersen, CERN/PS/BR/77-9, 7 march 1977.